

TIME DEPENDENT CRACK GROWTH IN QUARTZ
AND ITS APPLICATION TO THE CREEP OF ROCKS

by

RANDOLPH J MARTIN III

B.S., Boston College

(1964)

S.M., Massachusetts Institute of Technology

(1968)

SUBMITTED IN PARTIAL FULFILLMENT
OF THE REQUIREMENTS FOR THE
DEGREE OF DOCTOR OF
PHILOSOPHY

at the

MASSACHUSETTS INSTITUTE OF TECHNOLOGY

June, 1969 (i.e. June 1971)

Signature of Author.....
Department of Earth and Planetary Sciences, May 3, 1971

Certified by.....
Thesis Supervisor

Accepted by.....
Chairman, Departmental Committee on Graduate Students

Lindgren
WITHDRAWN
MAY FROM
MIT LIBRARIES

Abstract

Time-Dependent Crack Growth in Quartz
and its application to the Creep of Rocks

by

Randolph J Martin III

Submitted to the Department of Earth and Planetary Sciences May 3, 1971 in partial fulfillment of the requirements for the degree of Doctor of Philosophy.

The time-dependent growth of an axial crack in single crystal quartz tested in uniaxial compression with a constant load was studied as a function of temperature, stress and partial pressure of water. The time-dependent growth was found to obey an equation of the form

$$C - C_0 = At^n$$

where C is crack length, C_0 is the initial crack length at $t = 0$, t is time and A and n are constants. Typically as either the temperature, stress or partial pressure of water was increased, the rate of crack growth increased. The data was analyzed by comparing the relative times required for two cracks, with the same initial length, to extend an arbitrarily selected increment of 0.20 mm as one of the parameters was varied. The experimental results indicate that the changes in the rate of crack growth due to a variation in any of three variables could be treated independently and expressed by

$$\frac{t_1}{t_2} = \left(\frac{p_1}{p_2} \right)^{-0.95} \exp \left\{ \frac{25.8 \pm 0.6}{R} \left(\frac{1}{T_2} - \frac{1}{T_1} \right) + \frac{(\sigma_1 - \sigma_2)}{29.1} \right\}$$

where t_1 and t_2 are the times required for a crack to extend 0.20 mm at temperature T_1 and T_2 , stress σ_1 and σ_2 and partial pressure of water, p_1 and p_2 respectively and the subscript 1 indicates the initial value.

A relation between environment sensitive time-dependent crack growth and creep in brittle rocks is proposed. The increase in the rate of creep strain in rocks due to an increase in temperature or stress is shown to be consistent with the explanation of creep in terms of crack growth. Further correlations between static fatigue and the decrease in strength of brittle rocks with decreasing strain-rate and time-dependent crack growth are explored. The static fatigue of glasses, brittle rocks, and quartz is shown to obey a similar stress, temperature and moisture dependence as time-dependent crack growth in quartz. It is concluded that time-dependent crack growth is a principle mechanism in static fatigue of brittle materials.

The implications of time-dependent cracking as a principle mechanism in stick slip and stable sliding are also discussed. The transition from

stick slip to stable sliding is proposed to be a function of the rate of crack growth in brittle asperities on and near the frictional surfaces. Presumably at high strain-rates and low temperatures, stick slip is related to rapid crack growth primarily governed by the rate of increase in stress. At slower strain-rates, less than 10^{-7} sec⁻¹ or so, and higher temperatures the rate of crack growth is due more to stress corrosion and less to the rate at which the stress builds up. This may lead to stable crack growth and stable sliding.

Thesis Supervisor: William F. Brace.

Title: Professor of Geology.

TABLE OF CONTENTS

	PAGE
Title Page	1
Abstract	2
Table of Contents	4
Introduction	5
Deformation of Brittle Rocks	10
Creep in Brittle Rocks	13
Static Fatigue and Time-Dependent Crack Growth	14
Statement of Research Problem	17
Experimental Procedure	18
Experimental Results	31
Temperature Dependence	35
Stress Dependence	42
Partial Pressure of Water Dependence	51
Discussion	57
Analysis of Time-Dependent Crack Growth	57
Static Fatigue in Terms of Time-Dependent Crack Growth	64
Creep in Brittle Rocks	65
The Role of Crack Growth in the Creep of Brittle Crystalline Rocks	75
Creep Threshold	86
Strain Rate Dependence on the Strength of Brittle Rocks	88
Geological Applications	91
Presence of Water in the Crust	91
Fault Creep and Aftershocks	93
Stick-Slip and Stable Sliding as a Function of Time-Dependent Crack Growth	95
Fracturing Associated with Igneous Activity	100
Conclusions	101
Suggestions for Future Research	105
Acknowledgements	107
Bibliography	108
Appendix I:	111
Appendix II:	117
Appendix III: Tabulation of Data	125
Biographical Note	158

INTRODUCTION

One of the most striking characteristics of brittle rocks in laboratory tests is that at temperatures well below the melting point a continuous time-dependent increase in strain is observed when the rocks are subjected to a constant load. This implies that strain is not a single-valued function of stress at a given temperature and confining pressure, but depends on the time a specimen has been subjected to a constant load and on the magnitude of that load. This time-dependent deformation is called creep. It is possible therefore, to produce the same strain in a specimen either by loading to a high stress for a short time or a lower stress for a longer time. Similarly in constant strain-rate tests, the stress required to produce an axial or transverse strain is not a constant value but decreases with a corresponding decrease in strain-rate (Green and Perkins, 1968). This effect is also reported as a decrease of fracture strength due to a decrease in strain-rate, (Serdengecti and Boozer, 1961; Brace and Martin, 1968). This situation is not unlike that in the creep experiments where the stress required to achieve a single value of strain decreases as the length of time to achieve that value increases. It is possible, therefore, that in spite of the different loading regimes, a similar mechanism is responsible for the time dependency observed in these experiments. It seems advisable then to examine the operative deformation mechanisms in both constant strain-rate and creep experiments to determine whether or not a common deformational mechanism exists and if such a mechanism can satisfactorily explain the observed time-dependent strains, in each type of test.

Figure 1

Idealized stress-strain curves. (a) stress versus axial strain; (b) stress versus volumetric strain (after Brace et al., 1966)

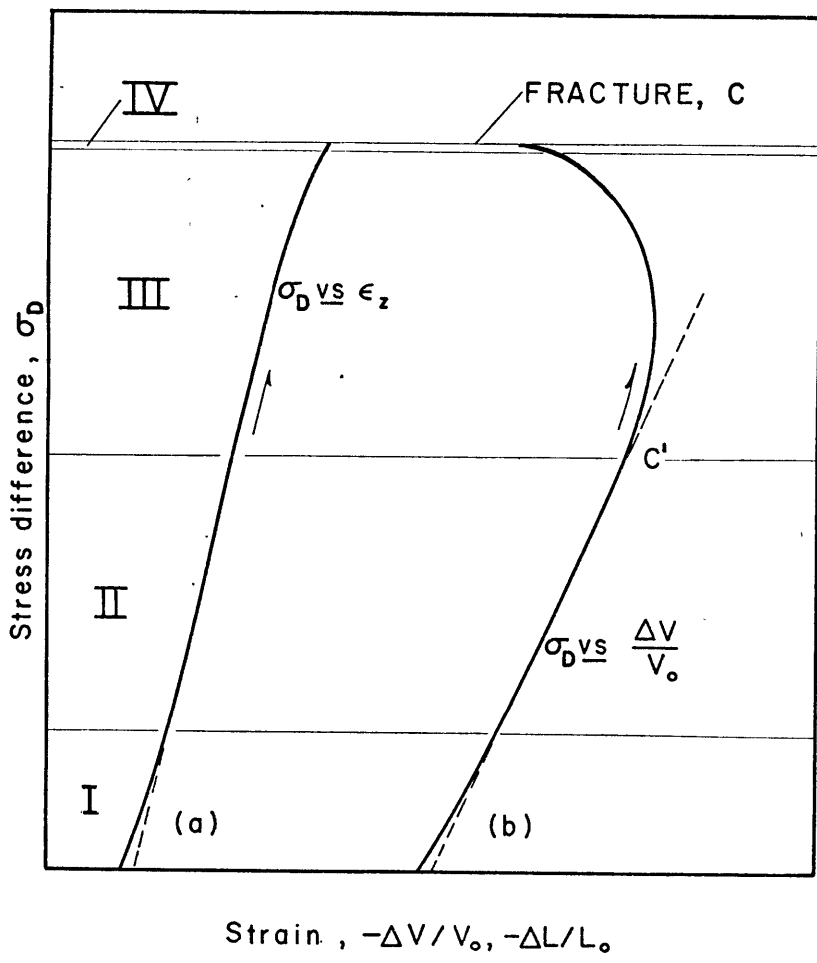
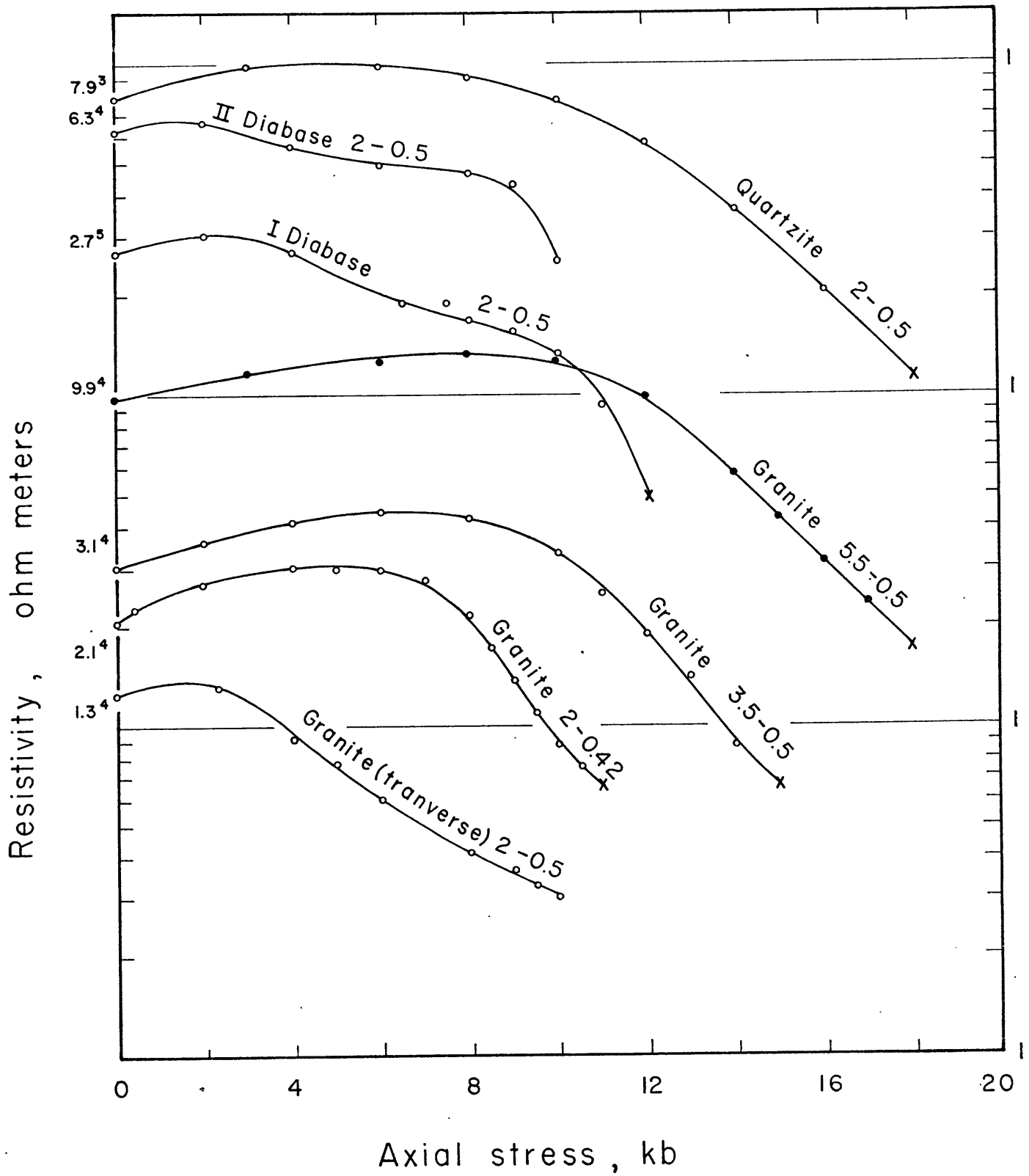


Figure 2

Decrease in resistivity as a function of axial stress for typical brittle rocks at low confining pressures. The increase in volumetric strain versus stress is demonstrated in Figure 1 (after Brace and Orange, 1968)



DEFORMATION OF BRITTLE ROCKS

The deformation of brittle rocks differs markedly from that of metals. While the deformation of ductile metals is accompanied by an exceedingly small or no permanent change in volume, the deformation of low porosity crystalline rocks exhibits an appreciable increase in volume prior to failure. Matsushima (1960 b) noted that during compression tests on granite the longitudinal strain was nearly linear with increasing stress. The lateral strain increased non-linearly with stress with the greatest strain occurring beyond half the compressive strength. Similar effects have been observed on norite and quartzite (Bieniawski, 1967) and tonalite (Green and Perkins, 1968). Brace et al. (1966) also observed inelastic volume increases during room temperature, constant strain-rate experiments on brittle rocks, even at high confining pressures. Based on these results, Brace et al. (1966) divided the stress-volumetric strain curve into four general regions (Figure 1). In regions I and II the rock behaves elastically (Brace, 1964); the toe in region I is due to the closing of pre-existing cracks (Walsh, 1965). Walsh also showed that the linear segment of the curve in Region II is due to elastic distortion of the mineral grains and slight relative shearing motion between grains due to the applied stress. Beyond one-half to two-thirds of the compressive strength, in region III, the volumetric strain increases relative to what would be expected if the material was elastic and continued to increase until failure. This inelastic increase in volume, called dilatancy, has been attributed to opening and subsequent growth of axial cracks.

Additional verification for the formation of axial cracks in region III is obtained by examining the changes in resistivity and compressional

wave velocity during deformation. In a brittle rock saturated with water, such as granite, nearly all the conduction is ionic, through the cracks and pores. Any change in the crack or pore geometry of the rock, will produce a corresponding change in resistivity. Brace and Orange (1968) observed that resistivity of typical crystalline rocks decreased by several orders of magnitude as the stress was raised to fracture; most of the decrease in resistivity occurred beyond one-half of the compressive strength when the volumetric strain began to increase (Figure 2). This result is consistent with the opening of axial cracks, because as axial cracks opened, the path for ionic conduction became less tortuous and the conductivity of the rock increased. Crack geometry also has a significant effect on compressional wave velocity; as the crack porosity increases the wave velocity decreases. Tocher (1957) and Matsushima (1960 a) observed the variation in compressional wave velocity in both the longitudinal and transverse directions during the deformation of brittle rocks. While the velocity in the longitudinal direction is relatively unaffected by stress, the transverse velocity begins to decrease at about half the fracture strength and drops by as much as 20 per cent in some cases prior to fracture. The decrease in transverse velocity is attributable to the opening of axial cracks.

Scholz (1968 a) took an auxiliary approach and examined the relation between microfracturing during deformation and volumetric strain. He found the frequency of microfracturing events was proportional to the inelastic volumetric strain and concluded that the observed microfracturing was due to cracking.

Experimental studies on cracks in glass and plastic plates have shown that inclined cracks do not extend in their own plane when the plate is

loaded in compression but form branch fractures at or near the ends of the inclined crack. These branch cracks grow along curved paths until they become parallel to the axis of compression, (Brace and Bombolakis, 1963; Hoek and Bieniawski, 1965). As the stress is increased the cracks continued to extend stably in the direction of the greatest compression. In rocks an inclined grain boundary may serve as a suitable source to initiate axial cracks. Brace et al. (1966) suggest several additional ways that axial cracks may form. The simplest case is an isolated axial crack opening due to the application of stress. Another possibility is the intersection of three pre-existing cracks or grain boundaries, two inclined and one axial. Under axial compression, sliding on the inclined surfaces is accommodated by the opening of the axial crack.

Brace and Riley (1971) conducted uniaxial strain experiments on several brittle rocks. The axial stress was continually increased while the transverse strain was kept equal to zero by continually increasing the confining pressure. Even when the axial stress exceeded 20 kb, the rocks did not fail and when the sample was unloaded no permanent strain was observed. This suggests that when axial crack growth is inhibited, brittle, low porosity crystalline rocks will not fail. Hence, axial crack growth appears to be a prerequisite condition for the failure of brittle rocks and if dilatancy is prevented there can be no permanent strain.

All the experimental evidence strongly suggests that axial cracks develop in brittle crystalline rocks during deformation. It would be useful to know, however, if all the axial cracks formed at grain boundaries or whether intragranular cracks formed to any great extent. Wawersik (1968) studied the distribution of cracks in Tennessee marble and Charcoal Gray

granite as a function of axial stress. He observed that axial cracking was distinct beyond approximately 60 per cent of the fracture strength and that intragranular splitting was dominant in this region. In the granite, the cracking was most prominent along cleavage planes in the plagioclase. Peng (1970) studied the fracture of Chelmsford granite in uniaxial compression. He examined polished sections of the specimens and observed that the cracks that lengthen markedly are parallel to the axis of loading and cracks with other orientations do not lengthen appreciably. Koide and Hoshino (1967) examined the distribution of cracks in sandstone loaded in compression at confining pressures up to 1.5 kb. They reported that the orientation of cracks tended to concentrate parallel to the axis of maximum compression. Finally, Wawersik and Brace (1971) observed on brittle rocks tested that at low confining pressures, less than 0.5 kb, the cracks tended to be predominantly axial. However, as the confining pressure was increased, the population of high angle cracks between 5 and 30° to the maximum compressive stress, began to increase. Therefore, it appears that axial cracking is a dominant feature of the deformation of brittle rocks, especially as the fracture strength is approached.

CREEP OF BRITTLE ROCKS

Brittle rocks tested in creep beyond approximately half the compressive stress also exhibit an inelastic increase in volume. Robertson (1960) conducted creep studies on Solenhofen limestone and observed that the sample density decreased and hence the volume increased although the sample was appreciably shortened. Additional creep tests on granite (Matsushima, 1960b)

and eclogite (Rummel, 1968) indicate that at stresses greater than approximately half the compressive strength the magnitude of the lateral strain is greater than the longitudinal strain and the corresponding lateral strain-rate exceeds the longitudinal strain-rate. Wawersik (1968) examined polished sections of Tennessee marble and Charcoal Gray granite which had been tested in creep. He concluded that the time-dependent strains resulted from local axial cracking, and the cracking was identical in form to that which had occurred in unconfined compression tests at higher stress levels. It appears therefore that the inelastic volumetric strains observed in uniaxial and triaxial compression tests and in creep at high stress levels can be satisfactorily explained in terms of axial cracking.

STATIC FATIGUE AND TIME-DEPENDENT CRACK GROWTH

If the observed strain in brittle crystalline rocks is at least in part attributable to axial cracking, then a possible explanation for the time-dependent deformation in creep tests is time-dependent axial crack growth. The concept of time-dependent crack growth appears frequently in the ceramic literature and is commonly employed to explain such phenomena as delayed failure in glasses and a wide variety of brittle ceramic materials. When a glass is loaded in tension below its tensile strength it will fracture after some time interval and this interval decreases as the stress or temperature is increased. This delayed failure, referred to as static fatigue, has been attributed to stress corrosion at the tips of cracks. In a corrosive environment, the high tensile stresses at the tips of cracks accelerate the corrosion reaction, weaken the material locally and

thus permit the cracks to lengthen. For a glass in tension, where the Griffith criterion applies, the cracks will extend stably to a critical length and then propagate unstably, leading to failure of the specimen. The corrosive agent responsible for the static fatigue of glasses is water (Charles, 1959; le Roux, 1965). The time-dependent lengthening of cracks is due to the hydration of silicon-oxygen bonds at the tip of the crack. Since the hydration product is weaker than virgin material, the crack propagates. Moreover, due to the general nature of the reaction other silicates and oxides, which react with water, should exhibit a similar behavior.

Unfortunately the hydration reactions for various silicates and oxides are not known explicitly and therefore neither are the factors which influence the reaction. Nevertheless, it would be expected that the reaction and the rate at which it proceeds are determined by the local stresses at the tip of the crack, the temperature and the concentration of water. Weiderhorn (1968) measured crack velocity in soda-lime glass, loaded in tension using a double cantilever arrangement, as a function of these variables. He found that the crack velocity behaved as a thermally activated process with an exponential stress dependence. These results are in agreement with an analysis of crack growth based on rate of reaction theory (Hillig and Charles, 1965). Most striking however was the fact that increasing the water concentration significantly increased the crack velocity.

Charles (1959) measured the compressive strength of granite, single crystal quartz and several alkali silicates at two different environmental conditions. Specimens were tested in dry nitrogen and saturated water

vapor environments. In all cases those samples tested in the saturated water vapor failed at a lower stress than those tested in dry nitrogen. Generally the fracture stress in saturated water vapor was approximately 60 per cent of the fracture stress in dry nitrogen. Hence, it appears that environment-sensitive crack growth is consistent with many of the observed features in brittle ceramic and natural silicate materials. For example, in static fatigue tests as the stress is increased, the crack velocity increases, the time for the crack to reach a critical length decreases, and the sample fails in a shorter time. In constant strain-rate tests, the picture is not quite as clear and concise, especially in compression, but all the observed effects are in the correct direction if crack growth is responsible for the failure of the material. By decreasing the strain-rate or increasing the water concentration, the material should be weaker since there is either more time for cracks to extend at lower stress levels due to a decrease in strain-rate or an increase in crack velocity at each stress level due to a relative increase in water concentration. Therefore the material should exhibit a lower strength.

Scholz (1968 b) theorized that compressional creep in brittle rocks could also be explained in terms of microfracturing with the observed deformation attributed to time-dependent cracking. By considering the probability of static fatigue occurring in a series of elements, each acting independently and relating the strain to the failure of these elements, i.e., the cracking of each element, Scholz derived an equation which has the same form and stress dependence as that exhibited by brittle rocks in creep. Although Scholz's theory satisfactorily explains the observed effect and predicts the shape of the inelastic volumetric strain vs. time at a constant load, it does so without considering the detailed

behavior of propagating cracks. The exact nature and contribution of crack growth to creep in brittle rocks is not made entirely clear in this analysis.

STATEMENT OF RESEARCH PROBLEM

If brittle rocks creep due to the time-dependent growth of axial cracks, then it would be of interest to examine the time-dependent behavior of axial cracks in compression. Axial cracks can form either at grain boundaries or within individual grains. Although cracking of both types undoubtedly occurs, intracrystalline cracking appears to dominate beyond approximately 60 per cent of the compressive strength as discussed above. In light of this observation, it seemed appropriate to concentrate our efforts on the details of axial crack growth within individual grains or the details of axial crack growth within individual grains or crystals. Since it was not possible to observe an intracrystalline crack within the rock, it was necessary to study intracrystalline crack growth in an isolated single crystal. By introducing a crack in a single crystal and examining its behavior under a constant load, the nature of the time-dependent growth could be observed. Furthermore, since temperature, stress and moisture content influence the gross behavior of brittle materials, the effect of these variable on cracks growth should be of prime importance. Finally, it must be determined in what way axial crack growth in single crystals is related to crack growth in rocks and to the strains observed in brittle rocks prior to failure. For example, how is the time-dependent crack growth in single crystals related to the time-dependent strains observed during creep? Is the form of the time-dependent strain during creep

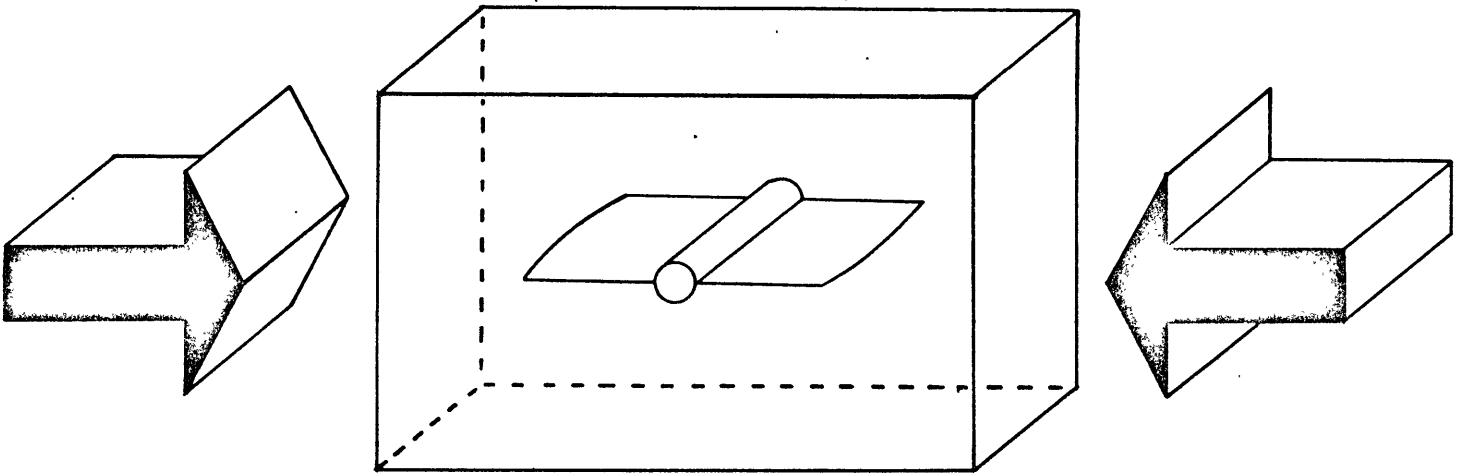
the same as that during crack growth? Are the temperature and stress dependencies the same for isolated axial cracks and strain in rocks? Is it possible to predict the creep behavior of rocks from the data obtained on axial cracks in single crystals? Can other time-dependent processes in brittle rocks be explained in terms of environment-sensitive time-dependent crack growth? With these problems in mind a study of the nature of axial time-dependent crack growth in silicates was undertaken.

EXPERIMENTAL PROCEDURE

Single crystals of quartz were selected for the crack growth experiments. Quartz has several features which make it ideally suited for this type of experiment. It has poor cleavage and behaves as a typical brittle material over a wide temperature range. It is necessary to select crystals that are free of cleavage since cleavage planes represent planes of relative weakness within the crystal and any crack intersecting such a plane may be deflected from its initial path and the rate of crack growth altered.

Brace and Walsh (1962) measured the surface energy of quartz and feldspar by propagating a crack in a cantilever loading device. They observed the crack surfaces in quartz were smooth and planar whereas the crack surfaces along cleavage planes in the feldspar were not smooth but made up of short segments, offset from one another and joined by short bridging cracks. Since cleavage planes may adversely influence the propagation of cracks in large single crystals, quartz seemed to be the ideal material. Furthermore, variations in composition between samples of the same silicate mineral are not uncommon and hence any comparisons of crack growth between samples

Figure 3 Schematic diagram of sample geometry illustrating axial crack radiating from a circular hole. Arrows indicate direction of uniaxial loading.

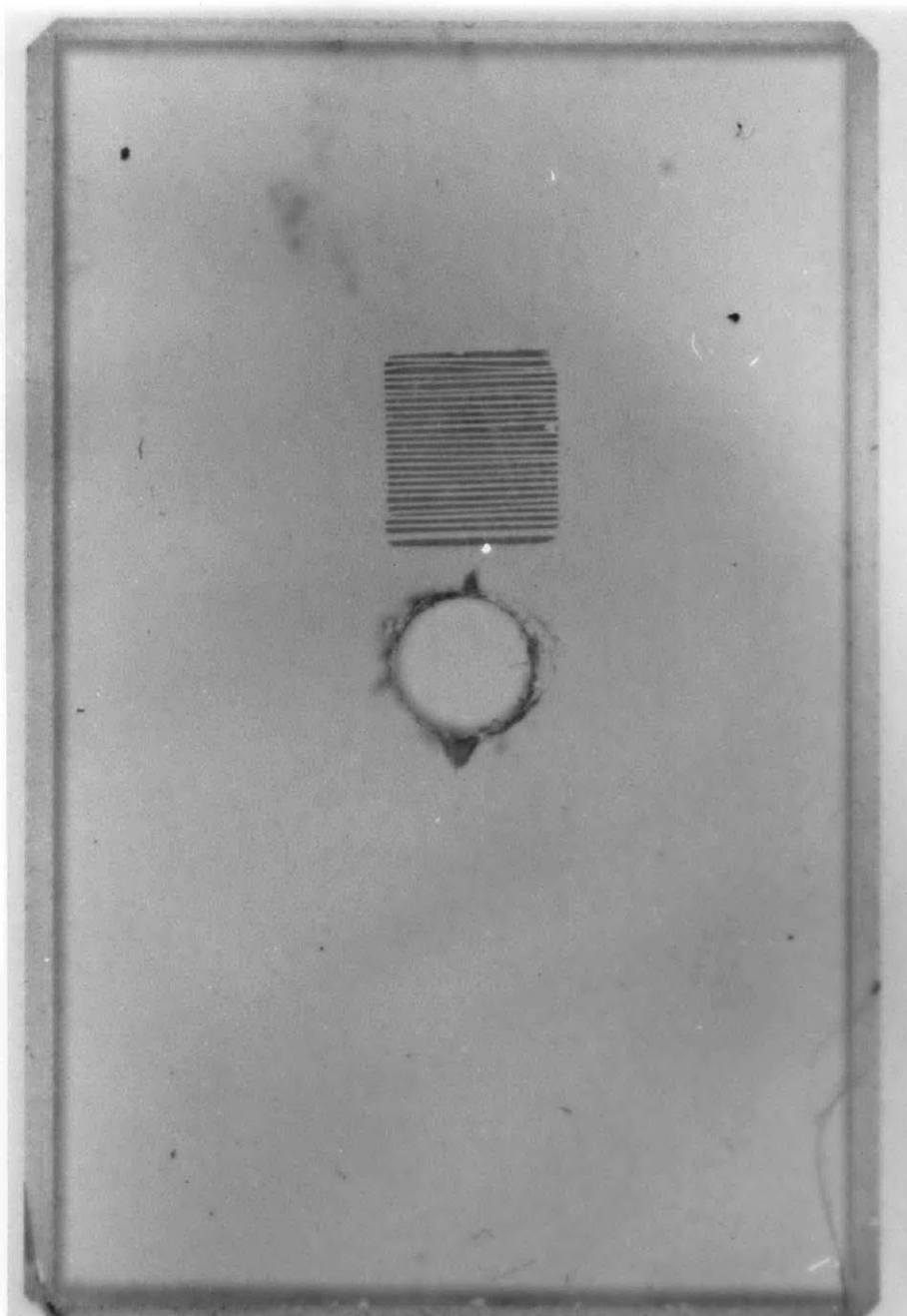


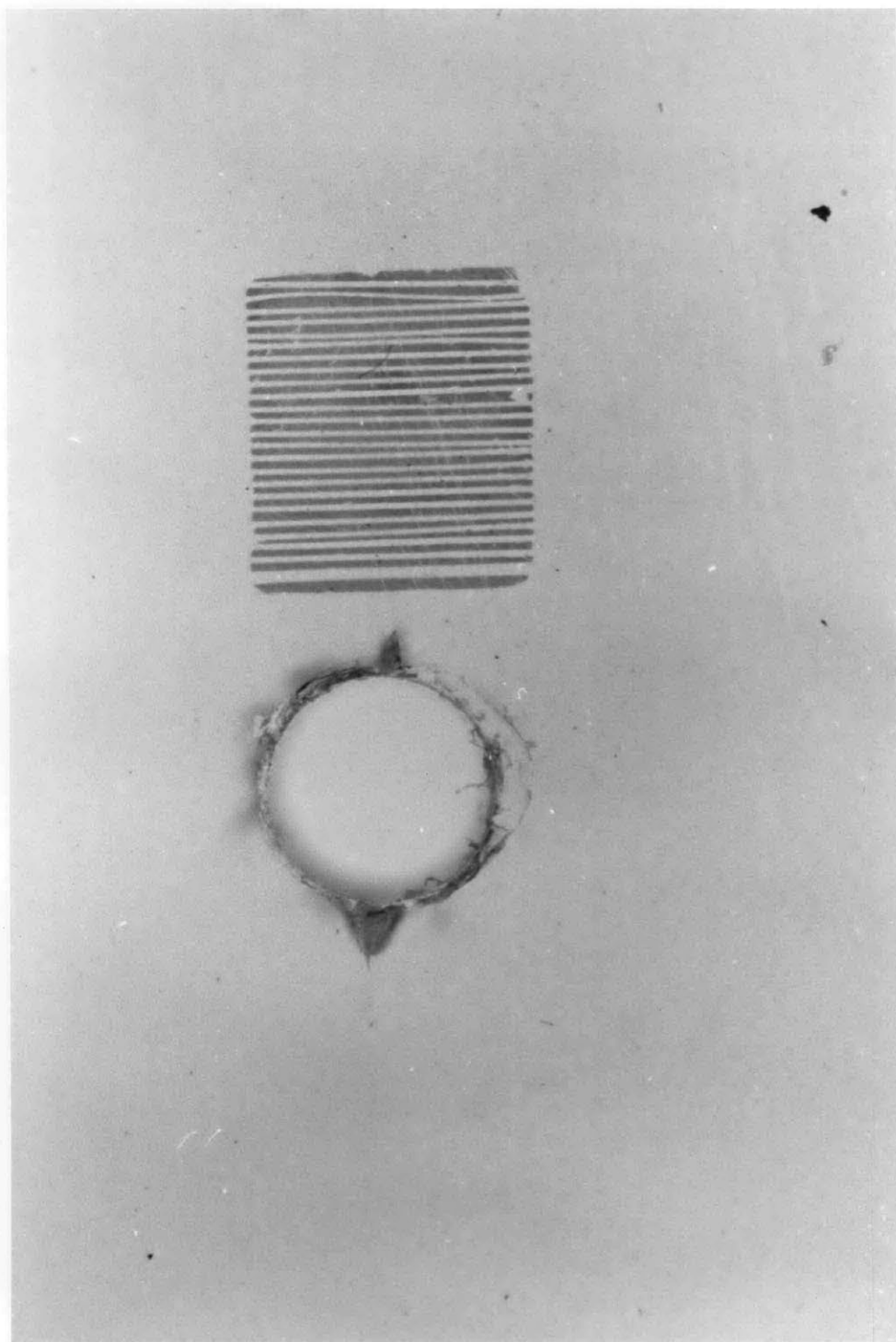
would be suspect unless a chemical analysis was performed on each sample to insure uniformity. The composition of quartz on the other hand, is constant except for small amounts of impurities. Although quartz differs from the other common rock forming minerals in that it lacks good cleavage and has a well-defined chemical composition, it is not unlike the feldspars, amphiboles and pyroxenes in that it possesses strong Si-O bonds. If it is these bonds that must be broken for a crack to propagate, then quartz, in this respect, is a typical silicate mineral and the logical choice of material for these tests. The quartz crystals were supplied by P.R. Hoffman Co., Carlisle, Pa. All the crystals were natural quartz.

The general approach in these crack growth studies was to introduce a crack parallel to the axis of loading in a crystal then to bring it to the desired environmental condition, to apply a constant compressional load, and to visually observe the change in crack length as a function of time. Unsuccessful efforts to measure crack growth with crack propagation gages are described in Appendix 1.

Prisms of quartz 3.18 x 2.03 x 1.27 cm. were ground square parallel. All the samples had a $+5^\circ$ X orientation. That is, the normal to the 3.18 x 2.03 cm. face is rotated 5° from $[1000]$ toward $[0100]$ in the (0001) plane. The long axis of the sample was within 5° of $[0\bar{1}10]$. The samples were then etched in concentrated hydrofluoric acid for two hours to blunt any surface cracks introduced by the grinding. In order to introduce the initial crack, a 3.18 mm. circular hole, which acted as a stress concentrator, was drilled normal to the 3.18 x 2.03 cm. face. When the sample was loaded in compression on the 1.27 x 2.03 cm. faces a crack parallel to the axis of compression formed (Figure 3). The plane of the crack was

Plates 1 and 2 Photograph of sample showing sample geometry and reference grid for locating the crack tip during time-dependent growth.





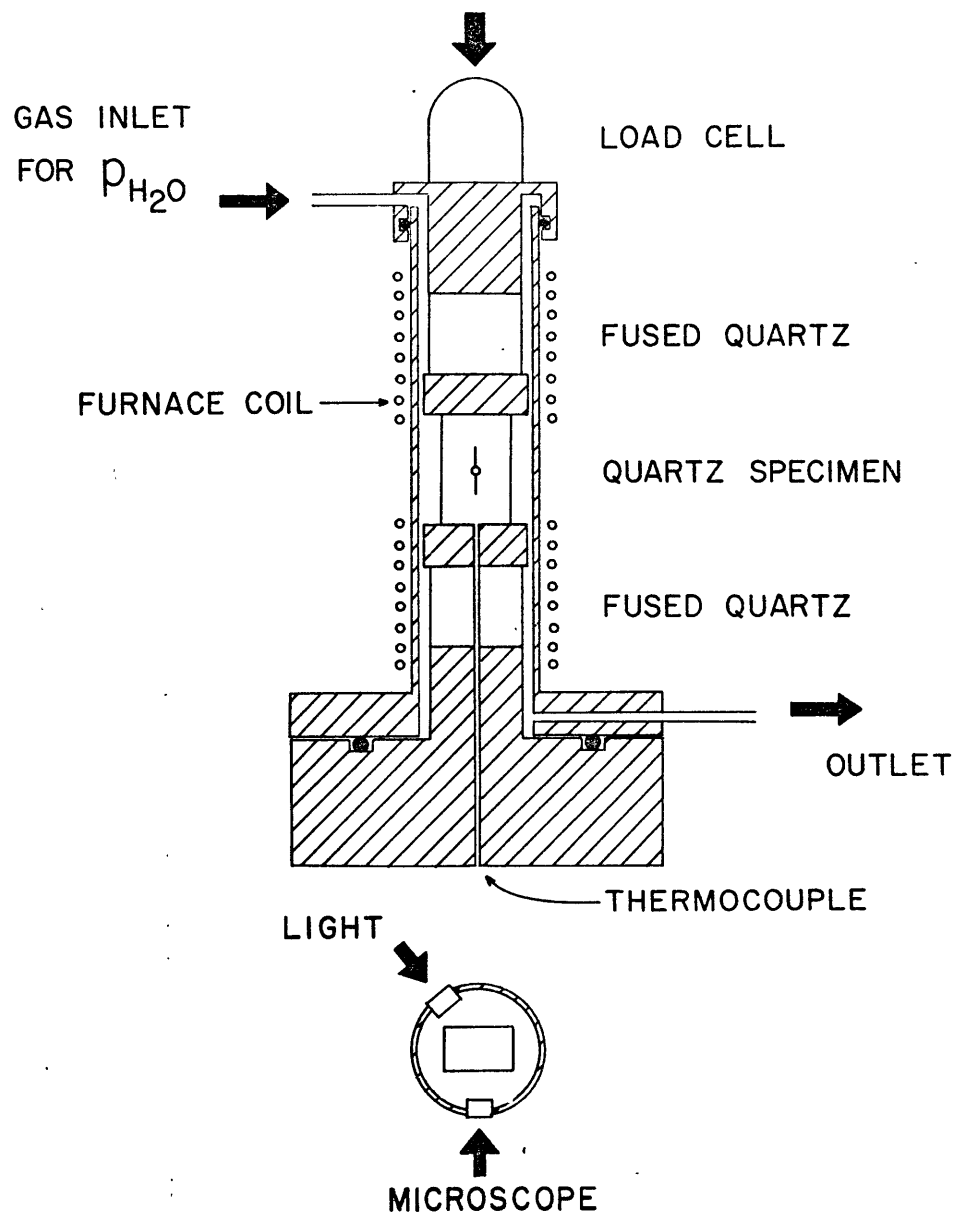
(0001) and the direction of growth was 5° to $[0\bar{1}10]$. By gradually increasing the stress the crack was extended to the desired initial length usually about 2.5 mm. from the surface of the hole. Since the measurements were made visually, it was necessary to have a reference grid along the path of crack growth. The surface normal to the axis of the drilled hole were polished and a grid composed of 25 thin gold strips approximately 0.10 mm. wide, separated by 0.09 mm., was deposited with the strips perpendicular to the direction of the crack growth. (Photos 1 and 2). The grid was obtained by evaporating several milligrams of gold over one polished surface which was partially masked with a free-filament strain gage. When the gage was removed the desired grid, appropriately located, remained. The exact width of each strand and inter-strand distance was then accurately measured using a microscope with a micrometer eyepiece.

A free filament strain gage was used because the spacing between each strand was the same and each strand had an identical width. Therefore, when the gage was removed from the sample after the gold was deposited, a uniform distribution of strips remained on the surface. The strips in Plates 1 and 2 appear slightly irregular because the filaments of the strain gage were not bonded to the surface. During the evaporating process some gold was deposited under the filaments, where they were not in intimate contact with the surface, producing somewhat uneven strips. Moreover, since the strain gages were available in a variety of sizes, it was possible to experiment with various grid spacings and determine which one provided the maximum resolution of the crack length.

A sketch of the test apparatus and loading arrangement is given in Figure 5. The quartz samples were loaded in a stainless steel test vessel

Figure 5

Schematic arrangement of experimental apparatus and sample. Plan view, at the bottom, is a section through the two windows and the sample.



in which the environment was controlled by streaming air with a known water content through the system. An external furnace provided the temperature variations. Two fused quartz windows, sealed with O-rings, were located in the vessel so that the portion of the crack growing toward the top of the vessel could be observed. A plan view through the vessel shows the relative location of the two windows with respect to the position of the sample (Figure 4). The crack and the reference grid was observed with a microscope tube through one window. The other window permitted illumination of the crack. A microscope light was adjusted until the critical angle on the crack surface was obtained. At this point, a bright sharp vertical line extending the length of the crack and terminating abruptly at the crack tip was visible through the microscope. It was thus possible to observe the advance of the crack tip with respect to the reference grid as a function of time. Using this method it was possible to determine the location of the crack at any time to within 0.005 mm.

The water content in the test vessel was controlled by keeping the partial pressure of water in the air streaming through the system constant. Compressed air was passed through two partially filled flasks of water, connected in series and immersed in a constant temperature bath. A manometer was tied into the system and the air pressure was regulated so that the pressure in the system was 4 mm. of Hg. greater than atmospheric pressure. As the gas passed through the flasks the partial pressure of water in the air adjusted itself to the equilibrium partial pressure over water at that temperature. When the temperature of the bath was below 0°C , the equilibrium partial pressure of water was reported as that over ice at that temperature. The temperature of the bath was constant to within

0.2°C from -28°C to 85°C. The temperature could be lowered even further to -76°C and held constant by filling the bath with dry ice and acetone. The reported partial pressure for each test is that of the equilibrium partial pressure of water at that temperature and atmospheric pressure. The range of partial pressures of water obtained in this manner extends from 7.6×10^{-4} mb at the temperature of dry ice to 578 mb at 85°C. In addition, by sealing the top of the vessel with a solid plug with an O-ring seal, and attaching the outlet port to a diffusion vacuum pump in series, with a mechanical pump the system was able to be evacuated to 2.6×10^{-5} mb (total pressure) and maintained at that level for several days.

The temperature in the system was maintained with an external furnace wound with Kanthal A-1 wire. The temperature was regulated with a Harrel TC-304 controller using a 100 ohm platinum sensor. The temperature, measured with an iron-constant and thermocouple at the base of the sample, remained constant to within 1°C. The tests were conducted over a range of temperatures from 93°C to 244°C. A maximum temperature of about 250°C was imposed by the breakdown of the silicone rubber O-ring seals around the observation windows.

The temperature gradient along the center axis of the sample was measured by drilling a hole through the sample in the plane of the crack. A thermocouple was inserted into the hole from the top of the vessel and the difference in temperature between selected points along the axis of the sample and the base of the sample was measured. The temperature difference over the length of the sample ranged from 6°C and 100°C to 15°C at 250°C. Although the variation in temperature over the entire sample is moderate at high temperatures, it never exceeded 3°C over the portion

of the sample where the crack growth was observed, i.e. up to 5 mm. from the periphery of the hole used as a stress concentrator. All the temperatures reported are those at the base of the sample.

A constant dead weight was applied to the sample. A modified arbor press, with an extended lever arm from which two lead weights were suspended, provided a suitable loading system. Moreover, the load was adjustable without disturbing the system because the weights were readily moved along the bar on roller bearings in the brackets supporting the weights. This arrangement was capable of producing continuous loads up to 3000 kg. The force was measured with an external load cell. In order to insure uniform loading in the system, a hemisphere of the same diameter as the load cell was attached to the top of the load cell. This provided point contact between the line of elements in the test vessel and the loading system and helped reduce any inhomogeneities in loading. Using this arrangement the total applied force was reproducible. The measured force was accurate to within 2 per cent.

The procedure in each test can be summarized as follows. All the loading elements and the sample were assembled in the test vessel. Then an initial crack was introduced in the crystal and extended to the desired length by loading the entire assembly in a hydraulic press at room temperature. The vessel was then placed in the arbor press, and the temperature was increased to the desired value. After thermal equilibrium was attained, air with a controlled partial pressure of water was continuously streamed through this vessel. The load was applied by rapidly lowering the weights, previously adjusted to produce the desired load, on to the experimental assembly. The increase in the crack length as a function of time

was observed through the microscope tube and recorded. Changes in the applied load during a run were accomplished by sliding the weights along the lever arm. Similarly, changes in water content in the test chamber were achieved by increasing the temperature in the constant temperature bath. In this way, crack growth under several loads and environmental conditions could be obtained on a single crystal.

EXPERIMENTAL RESULTS

The change in crack length as a function of time at the conditions examined can be approximated with an equation of the form

$$C - C_0 = At^n \quad (1)$$

where C is crack length measured from periphery of the hole, C_0 is the crack length at $t = 0$, t is time and A and n are constants. The results are summarized in Table 1. Typically, as either the temperature, stress or water content is increased, n increases. It should be relatively simple therefore to define n in terms of stress, temperature and water content and obtain a general equation for axial, time-dependent crack growth in quartz. The problem with this approach is that stress concentration factor at the tip of the crack is not constant but varies with crack length.

The stress distribution around a circular hole in plate in uniaxial compression is well known from elasticity theory. The stress concentration factor along the edge of the hole at 0° and 180° from the axis of compression is -1. This means that prior to the initiation of a crack a relative tensile stress exists at these two points equal in magnitude to

Table I

Summary of experimental results. Least squares fit to an equation of the form $C - C_0 = At^n$ is given in terms of the constants A and n. The last column gives a measure of the standard deviation of the data to a least squares fit.

TABLE I

Applied Stress bars	Partial Pressure of water mb	Temperature °C	Initial Crack Length mm	Duration Sec	A	n	$\frac{1}{N} (C - C_{calc.})^2$ $\times 10^{-3}$
1000	405	153	2.299	7.2×10^3	5.6×10^{-2}	.375	1.77
780	405	143	2.188	1.3×10^4	6.8×10^{-4}	.582	.196
930	405	200	2.576	1.5×10^4	1.24×10^{-2}	.377	.178
1000	405	93	2.525	7.5×10^4	2.98×10^{-2}	.286	1.23
1000	405	201	3.174	1.8×10^4	1.51×10^{-2}	.364	.232
1000	405	188	2.189	2.0×10^3	.111	.396	10.4
1000	405	184	3.666	9.2×10^3	8.89×10^{-3}	.324	.033
890	15.2	128	2.525	8.8×10^3	3.79×10^{-2}	.207	.045
890	60	128	2.787	1.3×10^4	3.14×10^{-3}	.551	2.20
890	113	120	3.264	1.1×10^4	1.20×10^{-4}	.743	.024
910	311 ⁻⁵	162	3.553	2.6×10^5	5.33×10^{-5}	.672	.285
1080	2.6×10^{-5}	135	2.4900	4.1×10^4	No observable Crack Growth		
910	(Vacuum) 7.6×10^{-4}	228	3.320	1.8×10^4	2.15×10^{-3}	.294	.002
910	6.1	235	3.520	7.5×10^3	1.16×10^{-2}	.273	.157
910	0.45	137	2.974	1.8×10^4	3.48×10^{-3}	.433	.403
910	6.1	137	3.182	6.9×10^3	1.94×10^{-4}	.863	.092

Applied Stress bars	Partial Pressure of water mb	Temperature °C	Initial Crack Length mm	Duration Sec	A	n	$\frac{1}{N} (C - C_{calc.})^2$ $\times 10^{-3}$
910	5.7	162	2.687	2.0x10 ⁴	7.16x10 ⁻³	.247	.011
910	0.45	188	3.195	6.8x10 ³	4.58x10 ⁻²	.313	.038
910	6.1	188	3.876	1.2x10 ³	2.65x10 ⁻³	.897	31.1
655	0.45	241	2.621	6.3x10 ⁴	9.19x10 ⁻³	.249	.098
740	0.45	241	2.779	1.2x10 ⁴	8.39x10 ⁻³	.376	.201
830	0.45	241	3.051	1.0x10 ⁴	6.13x10 ⁻³	.529	4.46
970	0.45	241	3.742	2.0x10 ⁴	1.48x10 ⁻²	.439	6.53
980	0.45	241	4.828	1.2x10 ⁴	6.79x10 ⁻⁴	.639	5.95
980	27.7	241	5.860	5.4x10 ³	2.64x10 ⁻³	.654	.228
525	405	244	2.781	1.1x10 ⁴	3.50x10 ⁻³	.460	.069
645	405	244	3.061	3.2x10 ³	6.05x10 ⁻³	.662	17.1
625	405	244	2.761	5.8x10 ³	1.49x10 ⁻²	.492	.680
625	405	244	3.775	5.8x10 ³	2.96x10 ⁻⁴	.856	1.45
695	405	244	4.178	2.6x10 ³	1.46x10 ⁻²	.594	.280
1000	405	100	2.001	4.6x10 ⁴	1.43x10 ⁻²	.347	4.37
1060	405	201	3.593	6.2x10 ³	.145	.276	.610
1000	405	100	2.200	3.9x10 ³	1.45x10 ⁻²	.377	.451

the uniaxial compressive stress. However, when the stress is increased to the point where an axial crack forms, the stress distribution around the periphery of the hole is altered and the tensile stress at the crack tip exceeds the magnitude of the applied compressive stress. When the crack forms it instantaneously extends approximately 1 mm. from the boundary of the hole and starts to undergo time-dependent crack growth. To extend the crack another one to two millimeters an additional increase in stress is required. This result indicates that the stress concentration factor decreases with increasing crack length. A detailed discussion of this point and an estimate of the relative change in stress concentration factor is given in Appendix II.

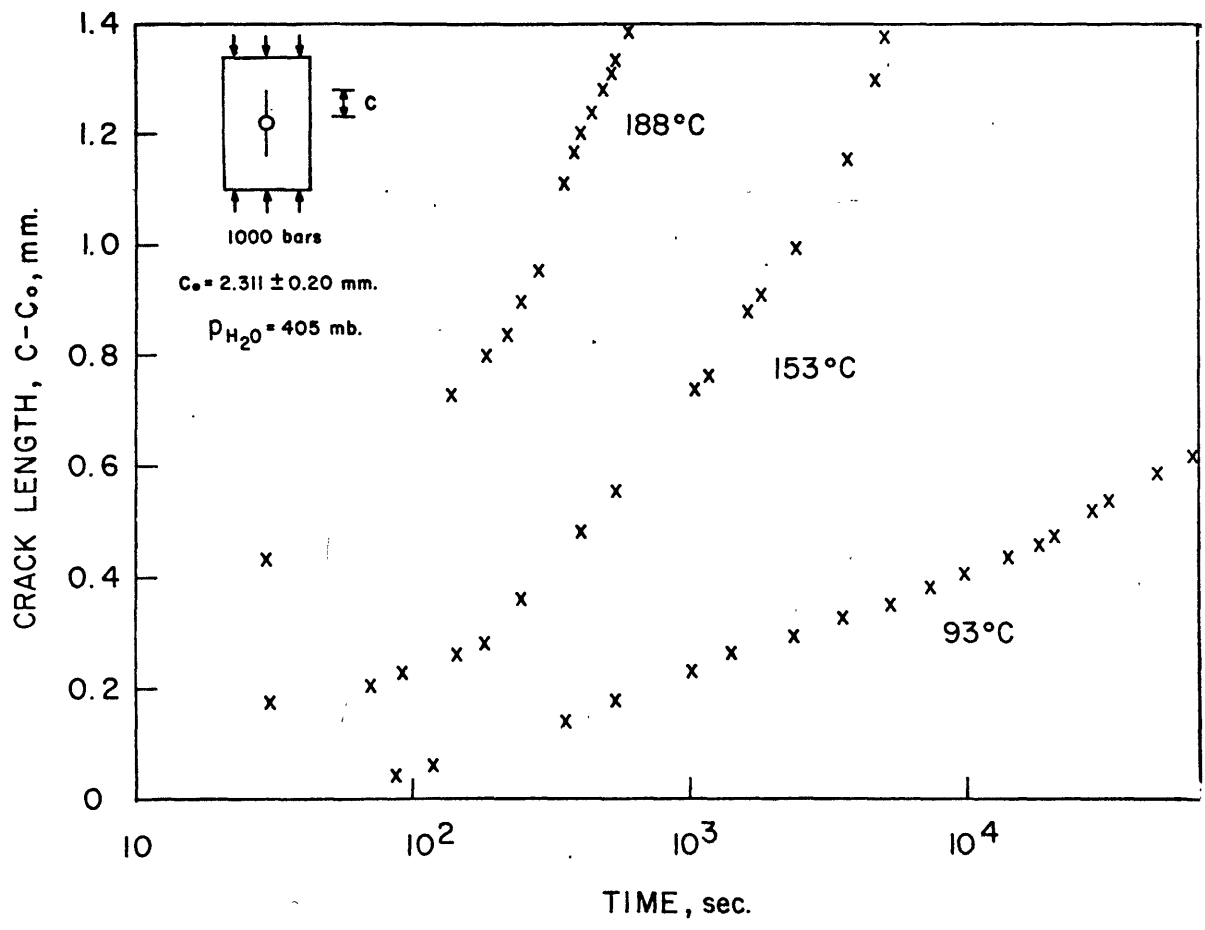
Since the exact variation of the stress concentration factor is not known, the dependence of the exponent, n , on temperature, stress and water content cannot be ascertained. However, the relative effect on crack growth due to changes in these variables can be determined by comparing tests with similar initial crack lengths, typically within 0.2 mm. Using this method of comparison, the difference in stress concentration factors between experiments is small, within approximately 3 per cent, the variation in stress concentration gradients should also be small and the results obtained will be meaningful.

TEMPERATURE DEPENDENCE

Figure 5 shows the effect of temperature on the rate of crack growths. Three samples with similar initial crack lengths, the same external stress 1000 bars, and partial pressure of water in the gas streamed by the sample,

Figure 5

Change in crack length with time at 93°C , 153°C and 188°C . The constant applied stress was 1000 bars and the partial pressure of water in the atmosphere surrounding the specimen was 405 mb.



405 mb, were tested at different temperatures. As the temperature was increased the rate of crack growth increased. This is reflected in an increase in the exponent, n , from 0.187 to 0.396 as the temperature was increased from 93° to 188°C .

The usual way of reporting the effect of temperature in a time-dependent physical process is to analyze the data in terms of an Arrhenus plot. In general, the rate of the process, v is expressed in terms of an activation energy, ΔF , by the relation

$$v = A \exp (- \Delta F/RT) \quad (2)$$

where T is absolute temperature, $^{\circ}\text{K}$, R is the gas constant and A is a constant. In these crack growth tests, the rate is best expressed in terms of crack velocity. Since the crack velocity continuously decreases with time a question arises as to the validity of this approach in this study. However, it is possible to analyze this effect as if it were a static fatigue test. Static fatigue is reported in time to failure at a constant load, and the onset of failure supposedly occurs when a crack or a series of cracks has extended to a critical length and compare the time for a crack to grow to that length under varying conditions. If the time for a crack to grow the same length, C^* , at two different temperatures, T_1 and T_2 , is t_1 and t_2 , respectively, Equation 2 may be rewritten as

$$\frac{C^*/t_2}{C^*/t_1} = \frac{t_1}{t_2} = \exp \left\{ \frac{\Delta F}{R} \left(\frac{1}{T_2} - \frac{1}{T_1} \right) \right\} \quad (3)$$

In short then, by taking the average crack velocity over an increment of crack growth, the data is in the appropriate form to obtain an activation

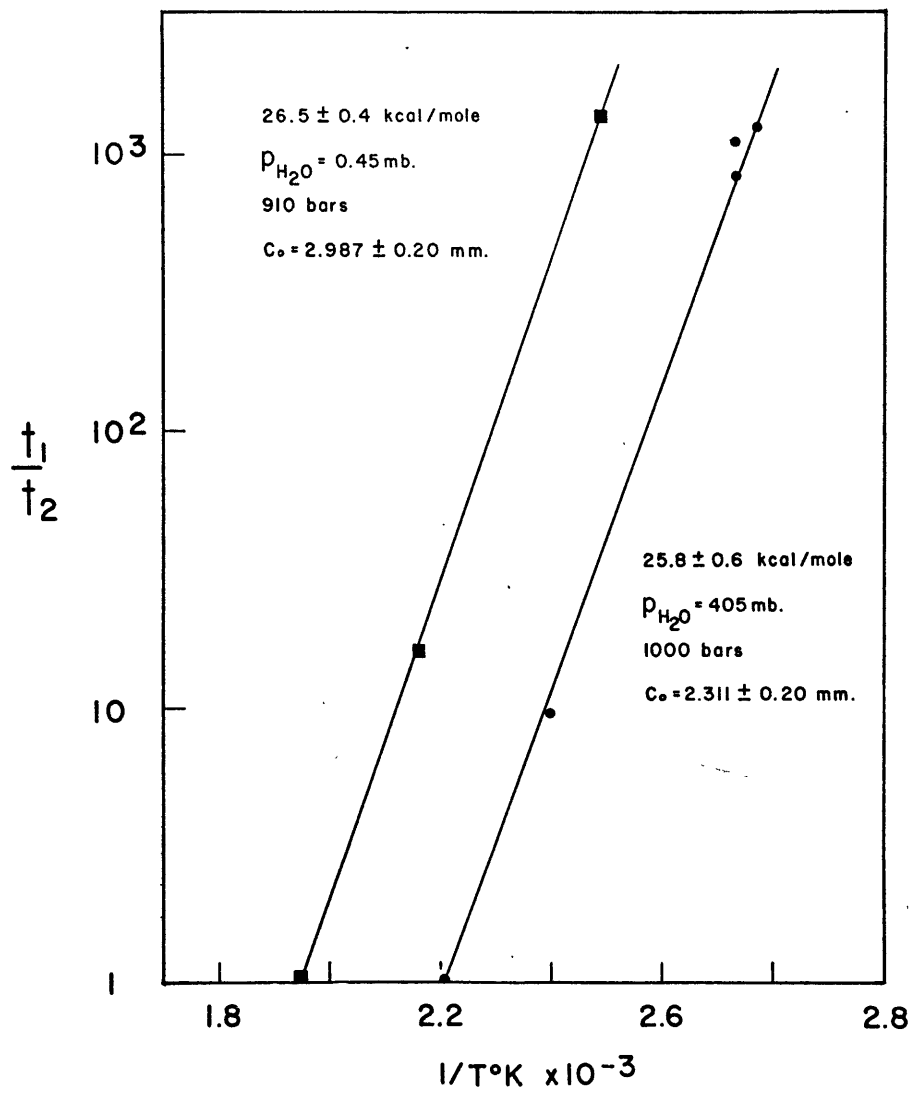
energy, if indeed crack growth is a simple, thermally activated process. It must be understood that this approach has been selected only so that a measure of the consistency of the data can be obtained and further comparisons can be made with existing creep and static fatigue measurements. Such an analysis is limited in that the activation energy is a function of the crack increment being considered.

The time for a crack to extend 0.2 mm. was selected as the variable to be analyzed. This value seemed appropriate for several reasons. First, the typical grain size of rocks in many laboratory tests is on the order of 0.2 mm. and second, this length permitted analysis of most of the data without extrapolating the observed results. There is no other particular significance attached to the value of 0.20 mm. In fact the data could have been analyzed as well using 0.50 mm., 0.02 mm. or any other value. If another value had been selected the apparent activation energy would change, increasing for longer increments and decreasing for shorter. Thus, the values for the activation energy reported are not in themselves as important as the fact that they can be expressed in the classical form of a thermally activated process.

Figure 6 is an Arrhenius plot of the ratio of the times for a crack to extend 0.2 mm. at selected temperatures vs. $1/T^{\circ}K$. By comparing each of the crack growth times to the test at the highest temperature more than two points per curve for each environmental condition were obtained. This was done for the data presented in Figure 2 and the points could be represented by a straight line whose slope corresponded to an activation energy of 25.8 ± 0.6 kcal./mole. The reproducibility of an experiment is also indicated in this plot by the scatter of the three points clustered

Figure 6

Determination of the activation energy required for
a crack to extend 0.20 mm.



near 100°C. The maximum error due to this scatter corresponds to 1.2 kcal./mole. The error associated with each data point is within the representation of the point in the figure.

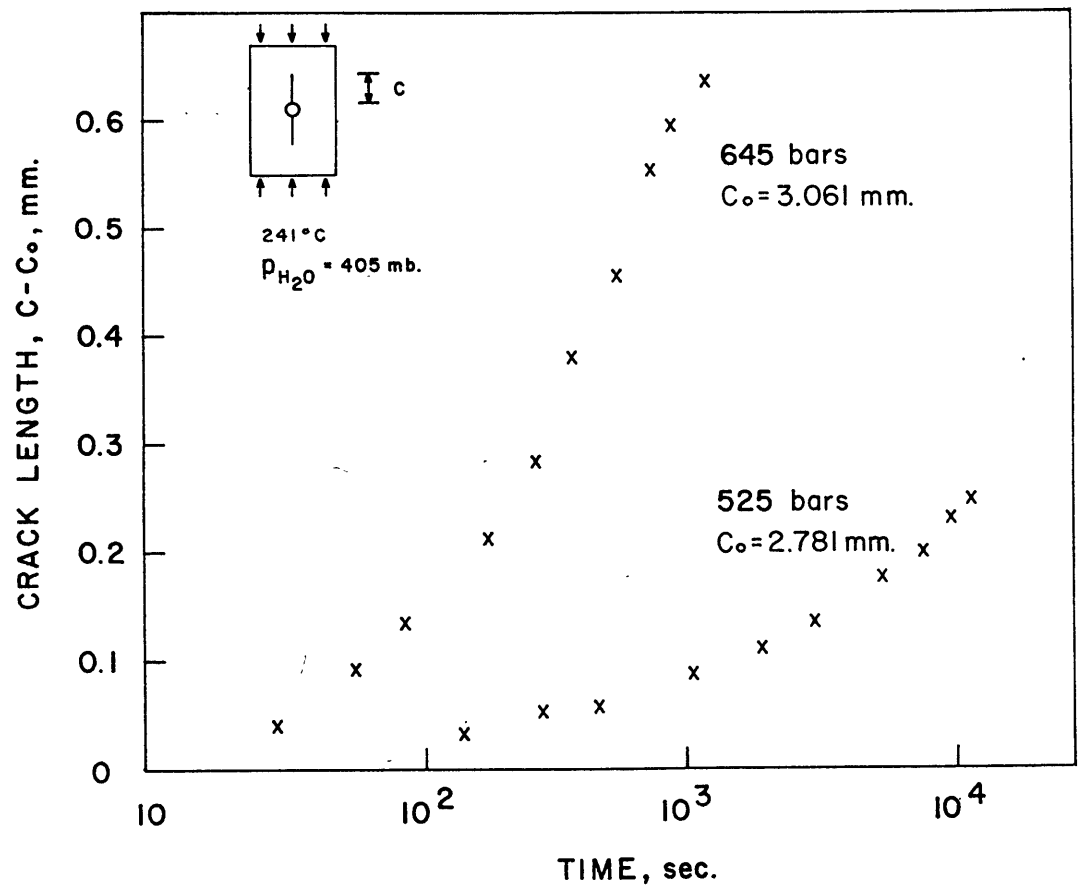
It was not immediately clear whether or not the effects due to temperature, stress, and water content were independent, at least to a first approximation. Therefore the activation energy for a series of experiments with a partial pressure of water of 0.45 mb. was computed. The activation energy obtained was 26.4 ± 0.4 kcal./mole. A stress correction was necessary in order to obtain at least three points. This correction is described below.

STRESS DEPENDENCE

The influence of stress on the rate of crack growth is shown in Figure 7. An increase in stress produces a corresponding increase in the rate of crack growth. To determine the stress dependence, a sample was loaded and the rate of crack growth observed. After a short increment of crack growth the stress was increased and a new rate was observed. The increase in load produced an immediate increase in the rate of growth. The data obtained by increasing the load was of the same form as that at the lower stress; that is, a power law. By examining the stress dependence with successive runs on the same sample, there was no variation in the other two controllable parameters, temperature and water content, and the possibility of variations between samples was eliminated. The data was analyzed in the same way as the temperature-dependence. The ratio of times for a crack to extend 0.2 mm. at two different stress levels was computed

Figure 7

Change in crack length with time at two applied stress, 525 and 645 bars, 241°C and 405 mb partial pressure of water.



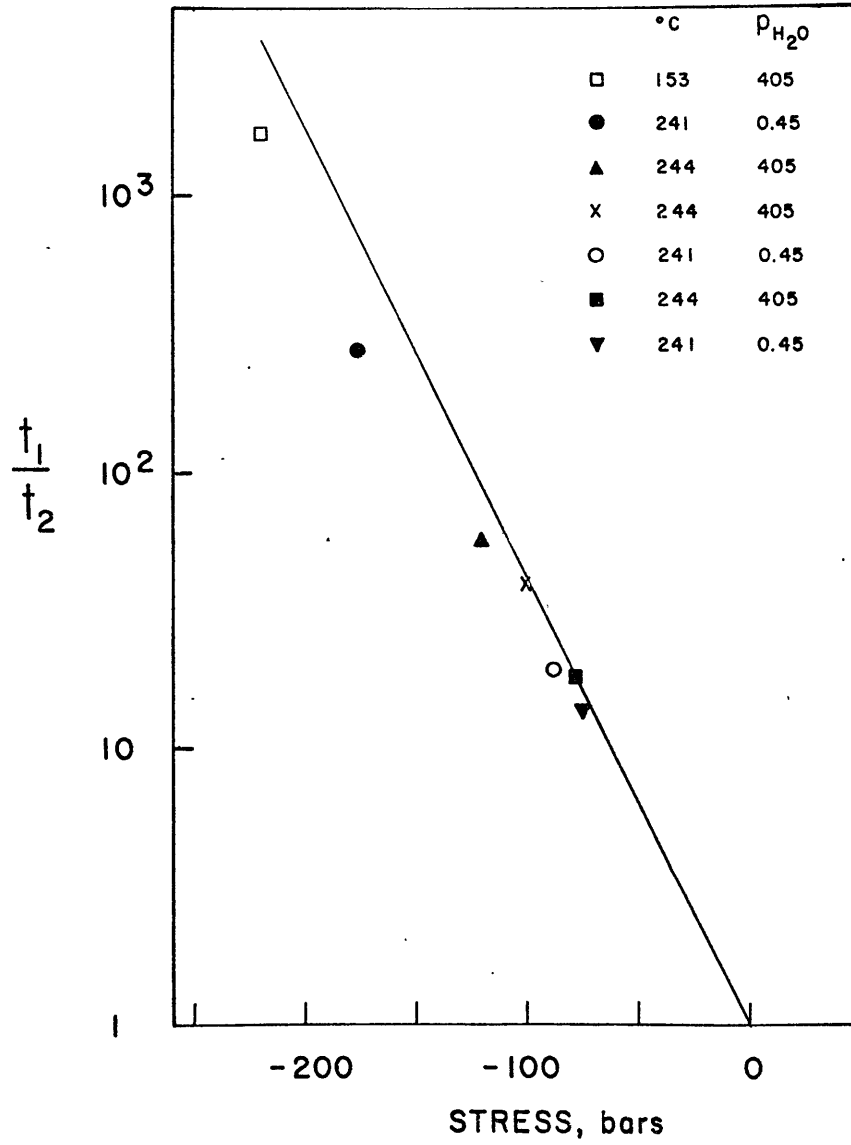
as a function of the stress increment applied. Once again it was necessary to determine the relative independence of the stress effect. Therefore, several experiments were carried out in the manner described above at various temperatures, water contents and stress levels. Since the absolute tensile stress at the tip of the crack was not known, all the data was plotted in terms of the increment of applied stress required to produce the change in the rate of crack growth (Figure 8). The data is best represented by an exponential stress dependence of the form

$$\frac{t_1}{t_2} = \exp \left(\frac{\sigma_1 - \sigma_2}{27.1} \right) \quad (4)$$

where σ_1 and σ_2 are the lower and higher stresses respectively and t_1 and t_2 are the corresponding times for a crack to extend 0.2 mm. The equation does not represent the best fit to the data. Due to the method of testing, the stress concentration factor decreased with successive tests on each sample. Therefore, the applied stress difference required to produce the observed change in the rate of crack growth is always greater than if both tests had identical initial crack lengths. Equation 3 reflects this fact. It is also apparent from Figure 8 that the stress dependence is independent of temperature, water content and stress level, at least within the limits of error in these tests.

One test of the data is to predict the behavior beyond the limits of the results and see if a consistent interpretation is obtained. In order to obtain three points to define an activation energy at a water content corresponding to 0.45 mb. partial pressure of water, a stress correction was necessary. Two tests were run at temperatures of 135°C and 186°C with

Figure 8 . Relative times required for a crack to extend 0.20
mm as a function of stress.

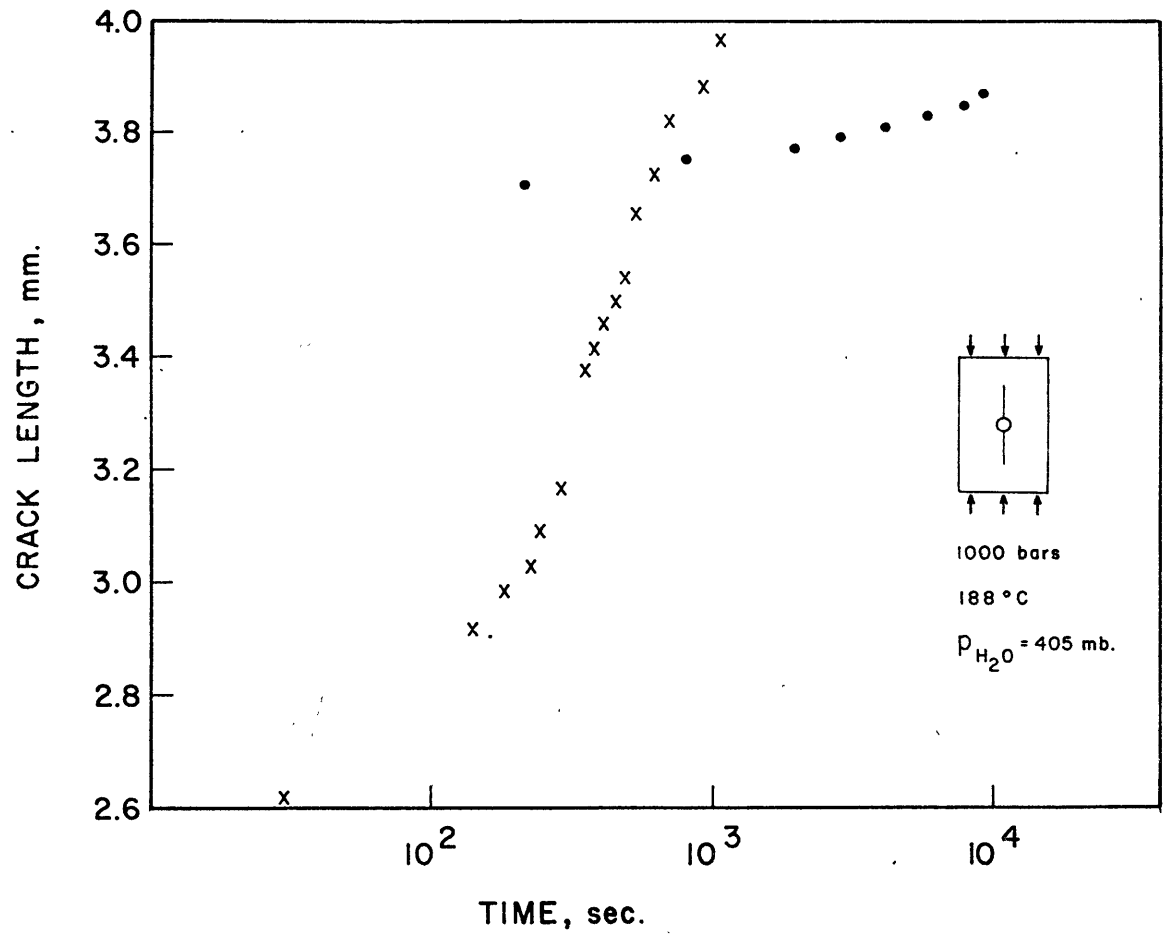


an applied stress of 910 bars. A series of stress-dependency experiments were conducted at 241°C but at stresses less than 910 bars. At 740 bars, the time for a crack with an initial length of 2.779 mm. to extend 0.20 mm. was 5×10^3 sec. It was necessary therefore to calculate the time at 910 bars. The new time for a crack to extend 0.20 mm. at this higher stress decreased to 9.5 sec. This value was used to compute the time ratios in Figure 6. The activation energy obtained was 26.5 ± 0.4 kcal./mole as previously noted. This value represents an upper bound to the activation energy because the initial crack length of 2.779 mm. was less than that in the other two samples and the stress at the crack tip proportionately higher. Hence the computed change in time to 9.5 sec. is a minimum and a time computed from a test with an initial crack length closer to the other two tests, 2.974 and 3.195 mm., would increase the computed time and decrease the activation energy. It appears therefore that it is possible to treat the effects due to stress and temperature independently and predict variations in the rate of crack growth due to changes in temperature and stress according to Equations 3 and 4.

One additional result was also evident in the stress-dependency tests. The rate of crack growth at any position along the crack is not strictly a function of the local stress at the crack tip, the partial pressure of water in the atmosphere surrounding the sample and the temperature, but is strongly influenced by previous history of the crack. This point is characterized in Figure 9; two curves obtained on two samples with similar external stresses, the same temperature and water content but different initial crack lengths intersect. At this point the stress at the crack tip is nearly the same for both samples. If the rate of change of crack

Figure 9.

Change in crack length with time at two different crack lengths. Temperature, applied stress and partial pressure of water in the atmosphere surrounding the specimen are the same for both experiments.



length is independent of the way this point is approached both curves should exhibit nearly identical slopes in this region. Since they do not, it appears that the rate of crack growth is also dependent on the previous history of any crack and not strictly on the external partial pressure of water, temperature and the local stress field.

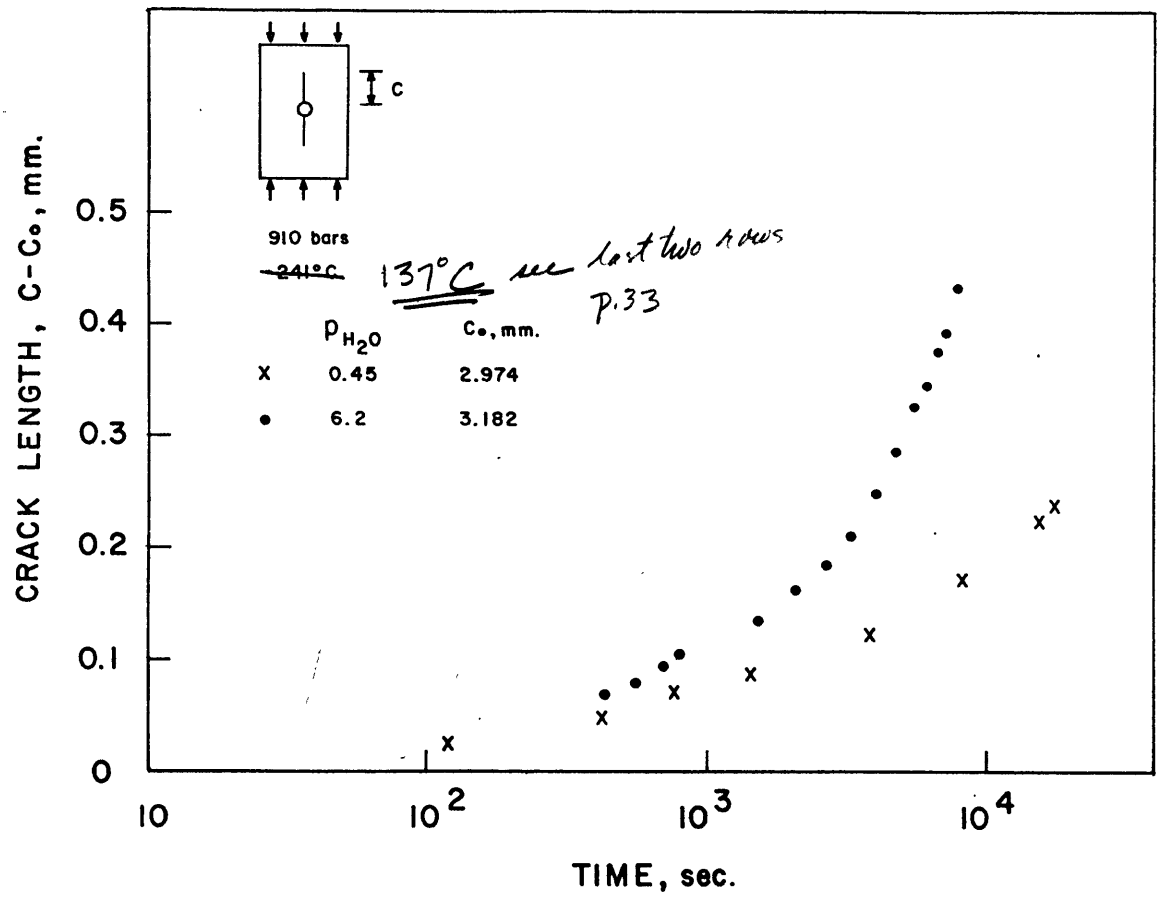
PARTIAL PRESSURE OF WATER DEPENDENCE

A typical change in the rate of crack growth due to an increase in water content in the atmosphere surrounding the crystal is shown in Figure 10. An increase in water content produces a corresponding increase in the rate of crack growth. The partial pressure of water dependence was determined in an analogous way to the stress dependence. The sample was initially tested at one set of environmental conditions. After the crack had extended several tenths of a millimeter, the moisture level was increased, while the applied stress and temperature remained unchanged, and the rate of growth observed.

The results were analyzed in the same way as the stress dependence. The ratio of time for a crack to extend 0.20 mm. during successive runs on the same sample at different water contents was determined as a function of the partial pressure of water in the test atmosphere. Moreover, to determine whether or not the effect was independent of stress and temperature, the results at several temperatures and stress levels were compared. Figure 11 is a plot of these comparisons; the moisture dependence for each pair of points was determined and then normalized to 1000 mb. The results fit an equation of the form

Figure 10

Change in crack length with time at two different partial pressures of water in the atmosphere surrounding the specimen.



$$\frac{t_1}{t_2} = \left(\frac{p_1}{p_2} \right)^{-0.95 \pm 0.05} \quad (5)$$

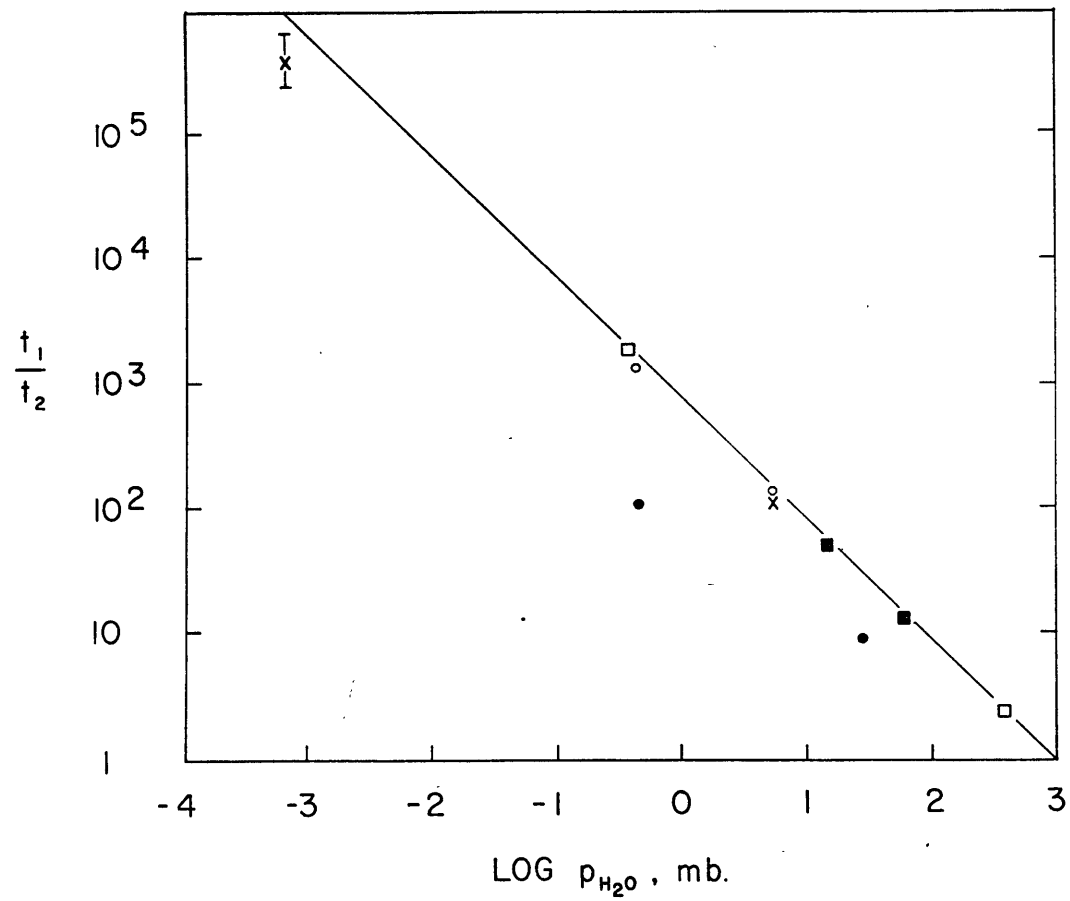
where t_1 and t_2 are the times for a crack to extend 0.20 mm. in an atmosphere with a partial pressure of water p_1 , and p_2 respectively and p_2 greater than p_1 .

The error brackets associated with the point at a partial pressure of 7.2×10^{-4} mb. indicates the possible error due to extrapolating the increment of crack growth to 0.20 mm. Furthermore, the equation is not the best fit through the data such as would be observed by a least squares fit. Since the stress at the crack tip decreases on successive tests even though the applied stress is held constant, the time for a crack to extend 0.20 mm. at the higher water content is longer than it would be if both had the same initial stress at the crack tip. Hence, the ratio of the times is less than what would be expected and the line has been drawn to reflect this situation. The two points that fall well below the line had a 1.03 mm. difference in initial crack length.

It appears therefore that within the experimental error, the effect of water content on the rate of crack growth can be considered independent of temperature and stress. Furthermore, since decreasing the water content decreases the rate of crack growth, it seemed likely that crack growth could be arrested in a high vacuum. Consequently, one test was conducted in a vacuum of 2.6×10^{-5} mb. total pressure; the partial pressure of water was not known. The sample was prepared in the usual manner. The test vessel was evacuated, the temperature increased to 135°C , and the sample was baked for two days. A load of 1080 bars was then applied. There was no observable crack growth, even after four days. By way of comparison,

Figure 11

The dependence of partial pressure of water in the atmosphere surrounding the specimen on the time required for a crack to extend 0.20 mm. ■ = 890 bars, 126°C; □ = 655 bars, 241°C; ○ = 910 bars, 137°C; × = 900 bars, 228°C; ● = 980 bars, 241°C.



a sample with a similar initial crack length, 1000 bars applied stress, 405 mb. partial pressure of water, 153°C extended over a millimeter in less than two hours.

Since each effect can be treated independently, a general equation incorporating all the effects studied can be written as

$$\frac{t_1}{t_2} = \left(\frac{p_1}{p_2}\right)^{-0.95 \pm 0.05} \exp \left\{ \frac{25.8 \pm 0.6}{R} \left(\frac{1}{T_2} - \frac{1}{T_1} \right) + \frac{(\sigma_1 - \sigma_2)}{29.1} \right\} \quad (6)$$

Equation 6 defines the relative change in time for a crack to extend 0.20 mm. due to variations in the partial pressure of water surrounding the specimen, the temperature and the applied stress.

The crack surfaces were examined under a microscope. The crack surface was not flat but conchoidal consisting of ridges and valleys. Over the total increment of time-dependent crack growth the distance between ridges was uniform, typically 2 to 4 microns. There was no tendency for the spacing to be larger during the initial stages of growth where the crack velocity was greater. The advancing crack was not normal to the direction of growth but slightly convex. The tangent to the crack front however, was normal to the direction of crack extension.

DISCUSSION

ANALYSIS OF TIME-DEPENDENT CRACK GROWTH

The experimental results indicate that time-dependent crack growth at a constant compressive load occurs in single crystal quartz in the presence of water vapor. Moreover, the rate of crack growth depends on the applied stress, the temperature, the partial pressure of water in the atmosphere

surrounding the crack, and the prior history of the crack. While the dependency of the rate of crack growth on temperature, stress and water content, was anticipated on the basis of results reported by other investigators, the effect of the previous history along the crack was not. This unexpected result appears to be advantageous, in defining the mechanism of time-dependent crack growth in compression as will be shown below.

The relative weakening of the quartz, reflected by an increase in the rate of crack growth with increase in water vapor content is consistent with the general theory of stress-corrosion in silicates. When a silicate material containing an axial crack is loaded in uniaxial compression a large tensile stress exists at the crack tip. The stress field in the vicinity of the crack tip represents an increase in the free energy of that region, and hence the region is thermodynamically unstable. If the increase in the free energy is great enough, the silicon-oxygen bonds at the crack tip will be broken, the crack will advance and will continue to advance until there is insufficient energy to break the Si-O bonds. However, if water is present, a smaller increase in free energy may be sufficient to permit the silicon-oxygen atoms to react with the water and form a hydrated silicate. Since a Si-OH bond is much weaker than Si-O bond, the crack will advance by breaking the weaker bonds. This is a very simplified and idealistic approach to the reaction at the tip of a crack, but we are limited in our analysis by fact that the exact hydration reactions are not known. It is likely though that the reactants, SiO_2 and H_2O in this study, will form intermediate, unstable species that will decompose to form the final reaction products (Charles, 1959).

The general theory of stress-corrosion as a mechanism of crack growth

has been developed by Hillig and Charles (1965). For a heterogeneous chemical reaction between a silicate or ceramic surface and corrosive environment, the rate of recession of the surface, v , will be proportional to the rate of reaction between the surface material and the corrosive agent. If ΔF is the activation energy required to form an activated complex from the reactants, then the velocity, v , is given by

$$v = v_0 \exp (\Delta F/RT) \quad (7)$$

where R is the gas constant and T is absolute temperature. The activation energy is considered to be stress-dependent. Hence, by expanding it in terms of a Taylor series as a function of stress, we obtain

$$\Delta F (\sigma) = \Delta F (\sigma=0) + \sigma \left(\frac{\partial \Delta F}{\partial \sigma} \right) \Big|_{\sigma=0} + \dots \quad (8)$$

where only the first two terms are retained. The first term is the activation energy of the chemical reaction at zero stress. The second term has the dimensions of volume per mole and has been termed activation volume; it is denoted by V^* . It is negative in this case since an increase in stress will tend to decrease the activation energy. Finally, since the roots of the crack are curved, and the curvature of a surface alters its free energy, this effect was also considered. The difference in free energy between a flat and curved surface is $\frac{\gamma V_m}{\rho}$ where γ is the surface energy, V_m is the molar volume of the solid and ρ is the radius of curvature of the surface. Since the effect of curvature will oppose the advancement of the crack it is subtracted from Equation 8. All of these effects may be summarized by rewriting Equation 7 as

$$v = v_0 \exp -(\Delta F_0 - V^* \sigma + \gamma V_m/\rho)/RT \quad (9)$$

Weiderhorn (1969) discusses the stress corrosion theory of Hillig and Charles in detail and introduces an environmental dependence. He considered a reaction at the crack tip between a gaseous species A and reacting species B in the material to form an activated complex B*. B is assumed to be proportional to the number of bonds in the solid so that as the reaction proceeds, the crack lengthens. Hence the rate of crack growth is proportional to the rate of the reaction. For one mole of B, the reaction can be expressed as



The change of free energy is

$$\Delta F_o = \mu_B^* - \mu_B - n\mu_A \quad (11)$$

where μ_B^* is the chemical potential of the activated complex and μ_A and μ_B are the chemical potentials of the species A and B respectively. If A is an ideal gas, and μ_B^* and μ_B are constant at constant temperature and total pressure then we can write

$$\mu_A = RT (\phi(T) + \ln p_A) \quad (12)$$

where $\phi(T)$ is some function of temperature, T, and p is the partial pressure of the species A and the crack tip. Substituting equations (11) and (12) in (9) we have

$$v = v_o A p_A^n \exp - \left\{ \Delta F_o - v^* \sigma + \gamma v_m / \rho \right\} / RT \quad (13)$$

where the constant terms have been incorporated into the constant A.

The generalized equation for environment-dependent crack growth is of the same form as equation (6) which is a measure of the average crack velocity over an increment of crack growth in quartz. Although our results appear to

be consistent with the theory developed above, a closer examination reveals several difficulties. Equation (13) refers only to the reaction at the tip of the crack. It does not attempt to describe the manner in which the water, in this case, is transported to the crack tip. Since the rate of crack growth in quartz is history dependent, it is also necessary to assess the factors which give rise to such dependency.

If we assume that Equation (12) describes the rate of reaction at the crack tip and the rate of reaction is proportional to the rate of crack growth, then the continuous decrease in crack velocity as the crack extends at a constant applied stress must be due either to a decrease in the partial pressure of water at the crack tip or a decrease in the local stress at the crack tip. The stress at the crack tip does indeed decrease as the crack lengthens but its exact contribution and magnitude is difficult to ascertain. What appears to be more important is that on two different specimens where the temperature and stress are the same at a given crack length, with the same partial pressure of water surrounding the sample, the crack velocities in the two crystals differ greatly. The remaining possibility is that the partial pressure of water at the tip of the crack is not the same as that in the atmosphere enveloping the crystal. This suggests that the rate of crack growth is limited by the rate at which water is supplied to the crack tip and not the rate of reaction.

The most apparent means of transporting water to the tip of the crack is diffusion along the axis of the crack. Diffusion tends to reduce concentration gradients and hence would transport water from the base of the crack where concentration is relatively high compared to the tip of the crack where the concentration is relatively low. As water is supplied to

the crack tip, the corrosion reaction occurs and the crack lengthens. The increase in crack length increases the path length for diffusion and thus the relative amount of water per unit time reaching the crack tip decreases producing a decrease in the rate of reaction and a corresponding decrease in the rate of crack growth. Although the diffusion equations appears to apply here, it is not possible to solve them exactly and then compare the rate at which water is supplied to the crack tip with the rate of crack growth. First of all, there are too many unknowns; for example, the diffusivity along the length of the crack is not known or even whether it is constant along the length of the crack. Furthermore, in this problem, the water concentration gradient is not the sole driving force for diffusion.

Diffusion acts to remove any free energy gradients, not only concentration gradients (Brophy, Rose and Wulff, p. 67, 1967). There is at least one other free energy gradient, besides the concentration gradient, along the axis of the crack and that is the free energy gradient associated with the strain energy. The strain energy due to the presence of the crack is greatest near the crack tip and decreases away from the crack tip. Moreover the magnitude of the strain energy should decrease as the crack length increases. Therefore, we can define at least two driving forces for diffusion but have no way of designating the relative contribution of each.

The activation energy determined from equation (13) is not strictly the activation energy of the reaction but the activation energy of the entire process: diffusion, reaction and any intermediate processes not

already considered. Furthermore, due to the method of obtaining the activation energy, it is not the activation energy at any time along the crack growth curve but merely an average over a given crack increment. Hence in our entire analysis we are comparing the times for two cracks with similar prior histories to extend a prescribed distance as one external parameter is varied. The time dependence merely reflects the fact that increasing temperature or stress produces a corresponding increase in the driving force for diffusion. When the partial pressure of water surrounding the crack is increased, there is an increase in the water concentration gradient and hence an increase in the rate of crack growth. Here the increase in water concentration is the additional driving force for diffusion.

The exponent in the environmental term of equation (6) is not the n in the reaction predicted by equation (10). The n in equation (10) is the quantity one would determine from the environmental term of equation (13) if the partial pressure at the crack tip is known. Since the partial pressure of water at the crack tip in our experiments varies with time and crack length, the value we obtain is determined over a range of partial pressures and does not represent the true value of n for the reaction. Moreover, n is defined in terms of the partial pressure of water in the atmosphere outside the crack, which we can only assume is proportional to the partial pressure of water in the crack, but do not know the actual value.

It seems clear that the rate of axial crack growth in quartz loaded in compression is limited by the rate at which water is transported to the crack tip. Once the reacting species reaches the crack tip the stress corrosion theory of Hillig and Charles controls the rate of reaction.

Although the two cooperating processes, have been arbitrarily separated the experimental coefficients of stress, temperature and partial pressure of water reflect an average value for the combined process over an increment of crack growth.

STATIC FATIGUE IN TERMS OF TIME-DEPENDENT CRACK GROWTH

The ultimate test of any crack study conducted in single crystals is whether or not it can be consistently utilized to explain phenomena observed in polycrystalline aggregates or single crystals with a random distribution of cracks. Scholz (1970) conducted a series of static fatigue tests in compression on single crystal quartz. He observed that the mean time for a sample to fail varied exponentially with stress. Since our data has been discussed in terms of the time required to extend a certain distance, and static fatigue is developed in terms of the time it takes a crack to grow to a critical length, the fact that both exhibit an exponential stress dependence is a strong indication that time-dependent cracking is responsible for static fatigue in quartz. Scholz also recorded the microfracturing during his tests and found that the cumulative number of microfracturing events vs. time obeyed a power law with an exponent between 0.3 and 0.8. Scholz (1968a) has previously established the fact that microfracturing events are related to cracking in rocks undergoing deformation. Since both crack growth in quartz and the number of microfracturing events during static fatigue of quartz can be represented by a power law in time, this is a further indication that crack growth during static fatigue is similar to crack growth in single crystal quartz. It appears then that

crack growth is not continuous but rather advances in jumps, each jump causing a microfracturing event, with these jumps related to the conchoidal nature of the fracture surface. Additional crack studies are planned to establish the relation between crack growth and microfracturing.

Scholz also observed that the rate of microfracturing increased when the sample was immersed in water and the failure rapidly ensued. This is consistent with our results if the rate of microfracturing is proportional to the rate of crack growth. By increasing the water content, the crack grows more rapidly relative to another sample at the same stress and temperature but at a lower partial pressure of water. The increased rate of crack growth produces an increase in the rate of microfracturing and the crack extends to a critical length in a shorter time than would be required at a lower water content.

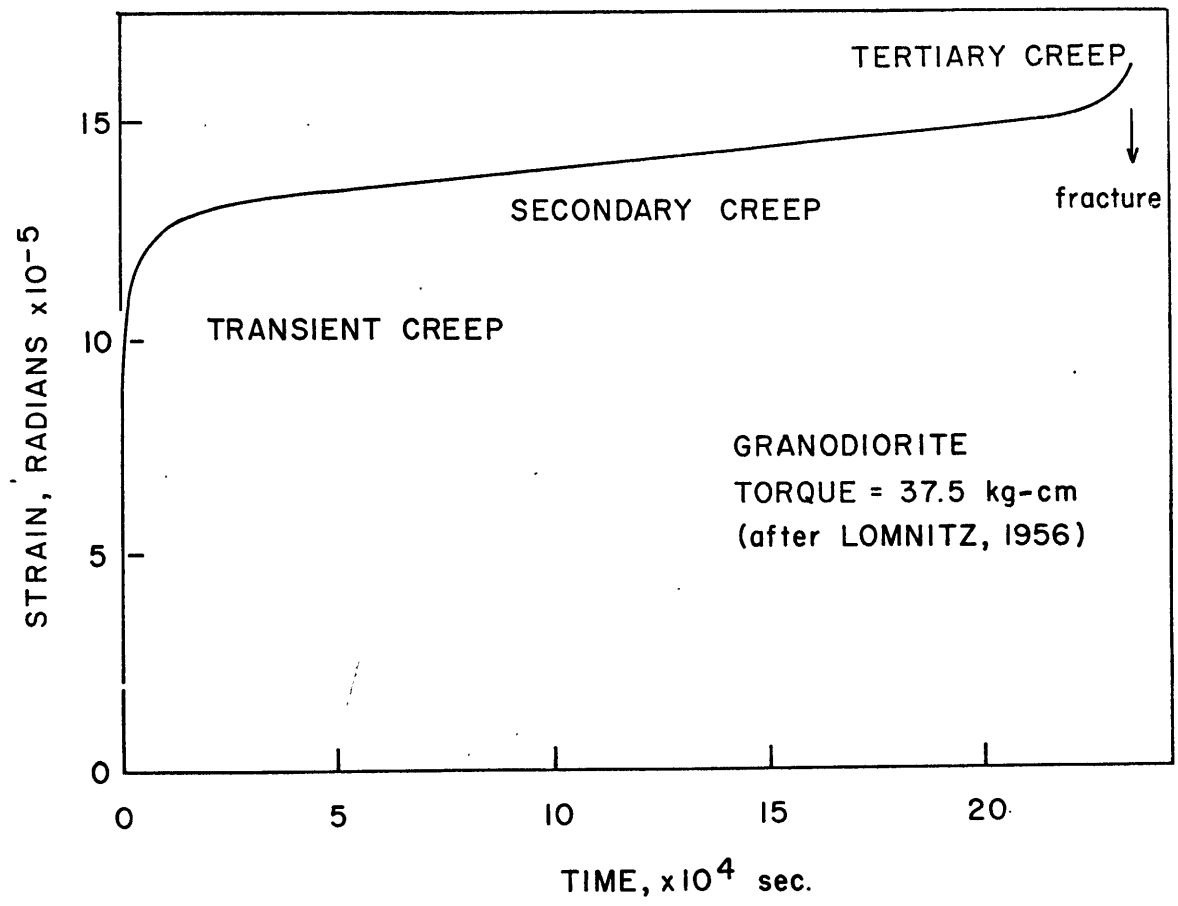
CREEP IN BRITTLE ROCKS

Next, it seems appropriate to examine the behavior of brittle rocks during creep and then to compare these observations with the results of the time-dependent crack growth study. Although only a limited amount of effort has been exerted on the study of creep in brittle rocks, sufficient data exists to rough out the general characteristics of rock creep. Creep can be defined as the time-dependent deformation of solids under a constant load. Typically, creep is reported in terms of three distinct phases, transient or primary creep, secondary or "steady-state" creep and tertiary creep or accelerating creep (Figure 12).

Transient creep has been reported for a variety of rock types over a

Figure 12

Creep strain in radians of granodiorite loaded in torsion to 37.5 kg-cm. This specimen exhibited all three stages of creep as indicated (after Lomnitz, 1956).



wide range of temperatures and pressures. The strain in this region decelerates rapidly with time and is often reported as proportional to the logarithm of time. Moreover, both the lateral and the longitudinal strains exhibit this logarithmic time dependence. At low stress levels, the rate of longitudinal strain exceeds that of the lateral. However, as the stress is increased the lateral strain-rate begins to increase relative to the longitudinal and eventually surpasses it at stresses approaching the fracture strength. Griggs (1939) measured the creep strain of Solenhofen limestone, loaded at approximately half its compressive strength, for over a year. He found that the total time-dependent deformation could be represented by an equation of the form

$$\epsilon = A + B \log t \quad (14)$$

where ϵ is the total strain, A and B are constants and t is time. Robertson (1960) studied the creep of Solenhofen limestone at confining pressures up to 4 kb. In each test the limestone displayed a primary creep stage in which the strain was proportional to the logarithm of time. Logarithmic transient creep stages have also been reported for micro-granodiorite, anhydrite, peridotite, sandstone, marble (Misra and Murrell, 1965), granite (Matsushima, 1960; see Figure 13), and eclogite (Rummel, 1968) tested in uniaxial compression at room temperature. Lomnitz (1956) conducted torsional creep tests on gabbro and granodiorite and found that the initial strain also obeyed a logarithmic creep law.

Unconfined creep tests on a wide variety of rocks have been reported at temperatures up to 750°C (Misra and Murrell, 1965; Rummel, 1968). The experimental results suggest that the primary creep phase can also be expressed in the form of equation (13).

Griggs (1939) and Lomnitz (1956) studied the time-dependent recovery of samples after the load was removed. Griggs found that the recovery of Solenhofen limestone obeyed an expression of the form

$$\epsilon = A - B \log t \quad (15)$$

where the terms are the same as defined for equation (13). Lomnitz studied the time-dependent recovery of gabbro and granodiorite which were originally loaded in torsion. He found an effect similar to that reported by Griggs but fitted his results to an equation of the form

$$\epsilon = A - B \log (1 - Ct) \quad (16)$$

where ϵ is the total shear strain in radians, A, B and C are constants and t is time. Over time intervals of the order of the initial creep test, nearly all the strain was recovered.

At low stresses transient creep may account for all the observed strain. However, at high stresses secondary creep is often observed. Generally in secondary creep, often called "steady-state", the strain is proportional to time. Figure 12 displays both transient and secondary creep observed in a granodiorite. Secondary creep has also been observed in granite (Matsushima, 1960b), ecogite (Rummel, 1968) alabaster (Griggs, 1939) and sandstone (Hardy, 1959). Typically secondary creep strain-rates in laboratory tests are on the order of 10^{-7} to 10^{-10} sec^{-1} and the rate of creep increases non-linearly with stress. The total deformation due to both transient and steady-state creep is usually fitted to an expression of the form

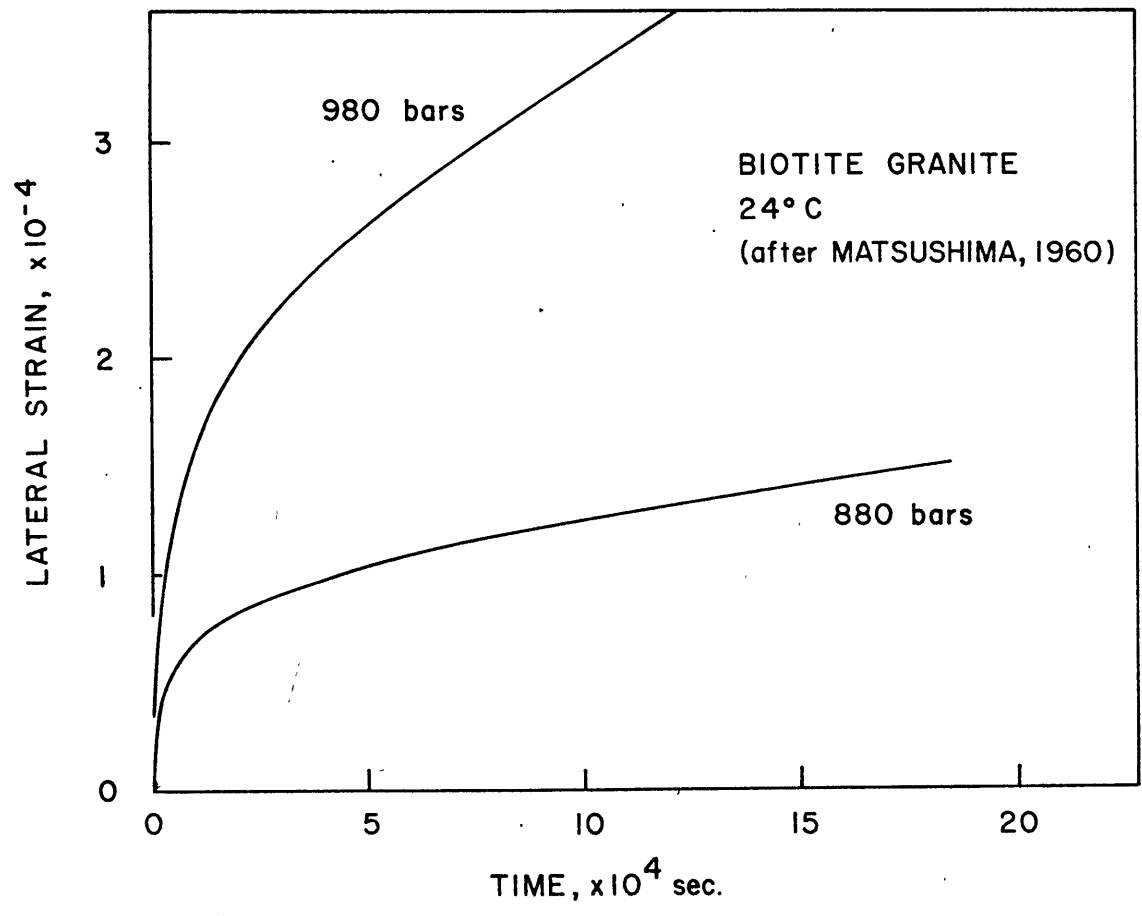
$$\epsilon = A + B \log t + Ct \quad (17)$$

where ϵ is the total strain, t is time, and A, B and C are constants.

If secondary creep is allowed to continue eventually the strain accel-

Figure 13

Effect of stress on the lateral creep strain in granite loaded in uniaxial compression at 24°C.



erates and the rock fails (Figure 12). All three stages of creep have been observed in granite (Matsushima, 1960; Rummel, 1968) and granodiorite (Lomnitz, 1956).

Wawersik (1968) noted that the fracture of brittle rocks tested in creep at stresses approaching the fracture stress was no different from that in a normal compression tests at room pressure or low confining pressures; that is, axial intracrystalline cracking was the dominant mode of fracture.

Robertson (1960) examined a progressive decrease in fracturing with increasing confining pressure. Below 1000 bars confining pressure, the samples were markedly fractured and had wide cracks, while above that pressure there were only fine cracks visible. At 4000 bars no cracks were visible. Measurements of the density change after the pressure was released also showed an interesting pressure effect. At confining pressures up to 2000 bars the sample densities showed a decrease on the order of 10 to 20 per cent; above 2000 bars the decrease was only about 1 to 2 per cent. Scholz (1968a) recorded the frequency of microfracturing in constant strain-rate tests on a marble as a function of confining pressure. As the confining pressure increased, the amount of dilatancy decreased and the frequency of microfracturing during deformation decreased. Above two kilobars the dilatancy disappeared even at 2 per cent axial strain. The observations of Robertson and Scholz have been interpreted as a change in the mechanism of deformation from brittle fracturing accompanied by dilatancy to plastic flow. Therefore, it is possible to observe similar transient and perhaps secondary creep stages on the same material at different confining pressures but the mechanism of creep may be entirely different. In

light of this, it is necessary to define a little more closely the range of temperatures and pressures over which creep is controlled by crack growth. Furthermore, since we are concerned primarily with creep due to crack growth in silicate materials, the implications of the transition from brittle to plastic behavior in carbonate rocks will not be pursued.

Experimental results on the deformation of granite and quartzite at high temperatures and confining pressures at a strain-rate of $5 \times 10^{-4} \text{ sec}^{-1}$ indicates that at temperatures between 500°C and 800°C at 5 kb these rocks show only limited plastic deformation and a much larger percentage of grain rupturing and fracturing (Griggs et al, 1960). In the granite, the biotite grains exhibited kink bands especially in the fracture zone. The quartz and feldspar were ruptured and the texture of the fracture zone was typically cataclastic. Similar tests on quartzite were conducted at 500°C and 5 kb. and analysis of the samples showed that fracturing of grains was still prevalent. A comparison of these samples with quartzites deformed at lower temperatures and pressures, indicates that there is twice as much fracturing in the quartz grains at 24°C and 1 kb. as there is at 500°C and 5 kb. Hence, fracturing is still a dominant failure mechanism in granite and quartzite at high strain-rates even at 500°C and 5 kb although other mechanisms of plastic flow may also occur.

Heard (1967) studied the deformation of Eureka quartzite at 500°C and 5 kb. as a function of strain-rate. At a strain-rate of $3 \times 10^{-1} \text{ sec}^{-1}$, the quartzite failed suddenly at a stress difference of approximately 24 kb., while at a strain-rate of $3 \times 10^{-7} \text{ sec}^{-1}$, the rocks began to exhibit ductile behavior at a stress difference of approximately 11 kb. At the high strain-rate, cataclasis was the dominant mode of failure with a large fault cutting

across the material, through and around the grains. At the lower strain-rate the material showed little internal fracturing of grains and the dominant mechanisms appeared to be intragranular slip. Heard and Carter (1968) studied the mechanisms of deformation in quartz and quartzite at confining pressures of 8 kb. and above, at temperatures of 500°C to 1020°C and at strain-rates of 10^{-3} to 10^{-7} sec⁻¹. They observed a discontinuous change in the predominant flow mechanisms with increasing temperature and decreasing strain-rate from basal slip and cataclastic flow through sub-basal lamellae slip to non-crystallographically controlled slip. Since all these observations were made at pressures in excess of 8 kb., it is not clear at what pressure and temperature, crack growth ceases to be the dominant mechanism of deformation at all strain-rates. Further experiments at lower confining pressures are needed to clarify the transition region from brittle to plastic deformation.

Goetze (1971) studied creep in granite, at confining pressures of 4 to 5 kb and temperatures up to the melting point (720°C) under small differential stresses, typically several hundred bars. The temperature dependence of creep was best fitted to an activation energy of 78 kcal/mole. Goetze concluded that such a large activation energy, compared to the activation energy for crack growth in quartz and static fatigue of quartz and silicate glass which fail due to cracking, is consistent with the diffusion of slower moving species within the constituent minerals. Furthermore Goetze considered extremely unlikely that crack growth was a significant mode of deformation at the conditions of his experiments.

Therefore, cracking as a mode of deformation and time-dependent crack growth as a principle mechanism of creep in brittle rocks appears to be significant only below 400°C to 500°C and at confining pressures below 4 kb.

The transition from creep due to crack growth to creep due to non-brittle mechanisms require further definition at temperatures near 400°C and confining pressures up to 5 kb.

THE ROLE OF CRACK GROWTH IN THE CREEP OF BRITTLE CRYSTALLINE ROCKS

Axial crack growth in quartz possesses several general characteristics that may be related to creep deformation. First, time-dependent cracking has an initial period of rapidly decelerating growth followed by what might be interpreted as a steady-state segment if the test is short (Figure 14). Furthermore, the velocity in this apparent steady-state region increases with stress and nearly vanishes at low stresses.

The similarity in form between the creep curve and that for time-dependent crack growth is in itself not sufficient to conclude that crack growth is the mechanism of creep in brittle rocks. What is needed is a theory of creep which defines the observed strain in terms of crack growth. Presently no such theory exists. It would be advantageous then to derive a relation between the rate of crack growth and the rate of deformation in a rock under a constant uniaxial load. Then, it would be possible to substitute reasonable values for the rate of crack growth into the relation and check whether or not the predicted strain-rates for rocks are in agreement with the published creep data.

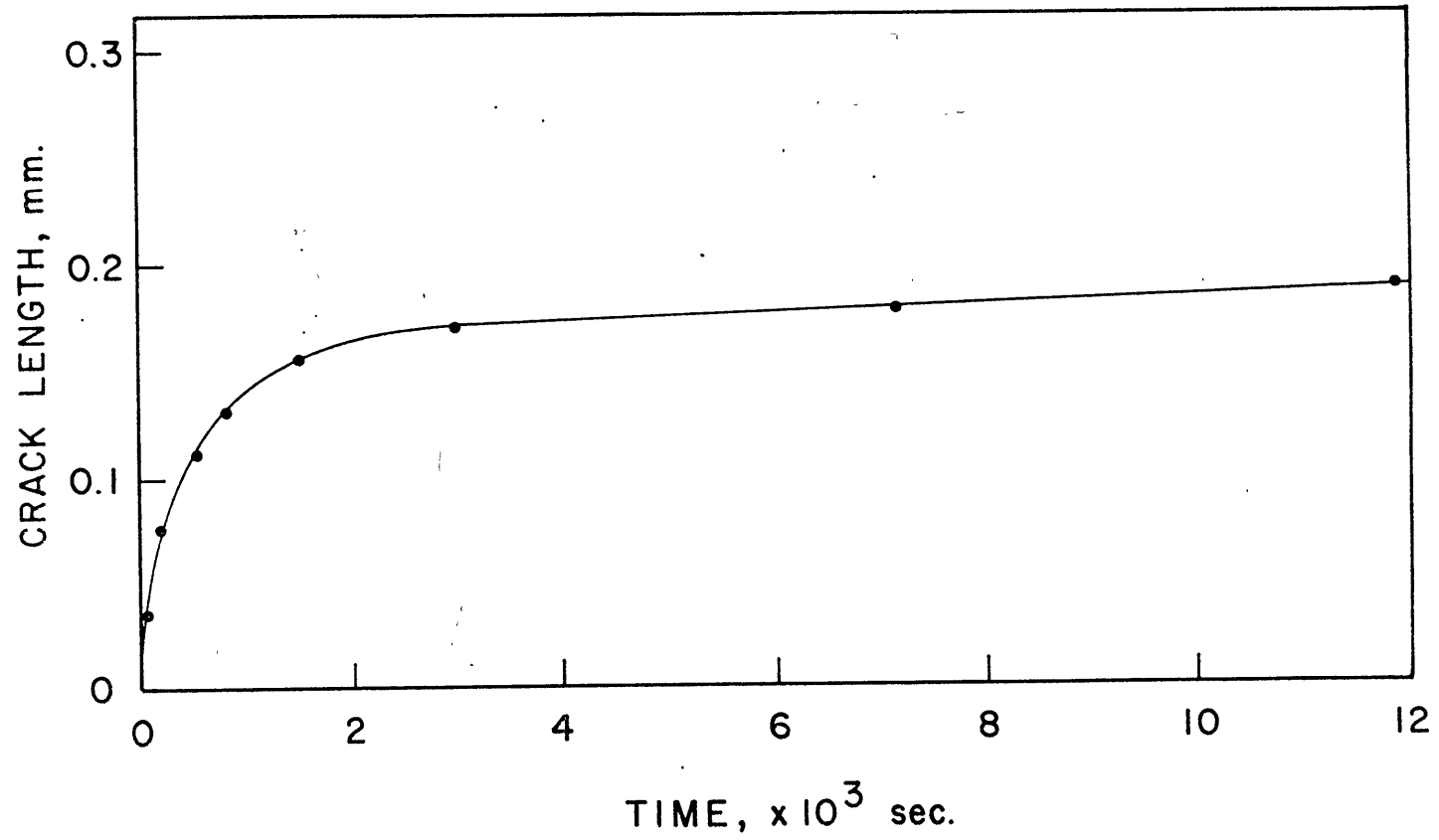
Walsh (1965) derived an equation for the effective modulus for a brittle material containing randomly oriented cracks. He found that the effective modulus, E_{eff} , in plane stress was given by

$$\frac{1}{E_{\text{eff}}} = \frac{1}{E} \left\{ 1 + \frac{4\pi\bar{c}^3}{3\sigma} \right\} \quad (18)$$

where E is the modulus of the elastic material surrounding the crack, \bar{c} is

Figure 14

Typical crack growth versus time curve, showing a transient stage and apparent constant crack growth rate over relatively short time intervals.



the average crack length and \bar{v} is the average volume of the region containing the crack. Expressing the modulus in terms of stress and strain, equation 18 becomes

$$\frac{\mathcal{E}}{\sigma} = \frac{\mathcal{E}'}{\sigma} (1 + AC^3) \quad (19)$$

where \mathcal{E} is the total longitudinal strain, \mathcal{E}' is the elastic strain, σ is the applied stress and $A = \frac{4}{3} \sqrt{\frac{1}{G}}$. Neglecting the elastic strain, as small compared to the total strain, and taking the logarithm of both sides yields

$$\log \mathcal{E} = \log \mathcal{E}' A + 3 \log C \quad (20)$$

Then by differentiating both sides with respect to time, we obtain

$$\frac{1}{\mathcal{E}} \frac{d\mathcal{E}}{dt} = \frac{3}{C} \frac{dC}{dt} \quad (21)$$

which relates the strain-rate in a rock to the rate of crack growth within the mineral grains and at the grain boundaries.

Equation (21) suggests that the stress, temperature and partial pressure of water dependence computed for crack growth should be similar to that for creep in brittle crystalline rocks. Consider two creep experiments on rocks with identical distributions of cracks at different conditions, either a difference in temperature, stress or partial pressure of water. The results for such a series of experiments can be analyzed in the same way as the results for time-dependent crack growth. By forming the ratio of the times required for each sample to achieve an arbitrarily selected strain, we have

$$\frac{t_1}{t_2} = \frac{\mathcal{E}_0 \sqrt{t_1}}{\mathcal{E}_0 \sqrt{t_2}} = \frac{\dot{\mathcal{E}}_1}{\dot{\mathcal{E}}_2} \quad (22)$$

where t_1 and t_2 are the times required for the samples to achieve a strain \mathcal{E}_0 and $\dot{\mathcal{E}}_1$ and $\dot{\mathcal{E}}_2$ are average strain-rates corresponding to t_1 and t_2 re-

spectively. Then by substituting equation (22) and (13) into equation (21) we have

$$\frac{\dot{\epsilon}_1}{\dot{\epsilon}_2} = \frac{\dot{c}_1}{\dot{c}_2} = \left(\frac{p_1}{p_2}\right)^n \exp\left\{\frac{\Delta F}{R}\left(\frac{1}{T_2} - \frac{1}{T_1}\right) + \frac{\sigma_1 - \sigma_2}{\beta}\right\} \quad (23)$$

where \dot{c}_1 and \dot{c}_2 are the average rates of crack growth corresponding to the times t_1 and t_2 required for a crack to extend a set increment of growth. Equation (23) suggests that the stress, temperature and partial pressure of water dependencies exhibited in single crystal quartz should also be observed in the creep of brittle rocks.

The question now arises as to whether or not the data on the rate of crack growth reported above is in a suitable form to be directly substituted into equation (23). Walsh (1965) derived equation (18) for the effective modulus assuming randomly oriented cracks with an average length, \bar{c} . As pointed out previously axial cracking is the dominant mode of deformation beyond approximately one-half the compressive strength. Hence, it must be determined to what extent a preferred orientation of cracks will affect the validity of equation (18). Moreover, the stresses in the vicinity of the cracks, both in the rock and in the single crystal quartz are not known. How then can the rate of growth of an isolated crack in a single crystal be compared with the observed strain-rate in a rock since small changes in stress greatly influence the rate of crack growth? It might also be asked whether or not the time-dependent crack growth measured in quartz is representative of what may be expected in other silicates, such as the feldspars, amphiboles and pyroxenes.

The difficulty that arises in applying equation (23) directly due to the predominance of axial cracks at stresses approaching the fracture

strength, can be overcome if axial crack growth also causes motion on cracks inclined to the axis of the applied stress. Consider the geometry discussed previously of the intersection of three grain boundaries or pre-existing cracks, two inclined and one vertical. Time-dependent growth on the axial crack may be sufficient to permit sliding on the inclined cracks or grain boundaries. In this way axial crack growth can contribute both to the longitudinal as well as transverse strain in a rock. Thus, if axial crack growth can activate motion on randomly oriented inclined cracks, equation (23) may be applicable and comparisons between the creep rate of rocks and the rate of axial crack growth can be made.

In spite of the possibility of this mechanism, the problem of the relation between the stress at the tip of an isolated axial crack in quartz and the stresses at the crack tips within the rock still needs to be clarified. Since it is not known how the distribution of stress concentration factors of cracks within a rock is related to the stress concentration factors for the isolated crack in a quartz crystal, a direct correlation between strain-rate and the rate of crack growth is not possible. In spite of this, several generalizations about the range of stresses involved in producing experimentally measurable variations in the strain-rate and rate of crack growth may help to define and limit the problem.

Crack growth in single crystal quartz can be expressed as a power law with a variable exponent (equation 1). By increasing the stress, the rate of crack growth increases as reflected by an increase in the exponent. In practice however, there is a limitation on how much the stress can be varied. If it is increased too much the rate of crack growth is so great that meaningful observations are not possible. For example, a crack that

extends approximately 2 mm in less than 10^3 sec. is growing too fast to measure accurately. In terms of a typical rock, suitable for laboratory tests, with grain sizes on the order of 0.5 mm. intracrystalline fracture would occur in several minutes and rock would fail shortly thereafter. On the other hand, if the stress is too low, no crack growth is visible over reasonable time intervals.

In rocks the situation is much the same. If the stress is too high the rock creeps at a high strain-rate and fails in a short time interval. When the load is small the strain is proportionately small and the strain-rate is extremely low. The variation in stress at a given temperature for which meaningful laboratory tests are possible is approximately 300 bars for the single crystals of quartz with the sample geometry described above and in the vicinity of several kilobars for most crystalline rocks at room pressure. The larger range in the stress variation for rocks is not unexpected. In a single crystal, comparisons of the rate of crack growth are always made between samples with similar stress concentration factors at the crack tip. In a crystalline aggregate the stress concentration factors may be much higher or much lower than for an isolated axial crack in a single crystal depending on crack geometry of the adjacent grains. In rocks then, the strain will be proportional to the number of cracks that have been activated as well as the rate of crack growth. As the stress is increased, a greater number of cracks will achieve the stress necessary to initiate significant crack growth. At very high stresses, approaching the compressive strength, a large proportion of the cracks are activated and growth is very rapid leading to failure in a short time. At low stresses, very few cracks are subjected to stress levels sufficient for crack growth to commence, and little deformation is observed.

It might be anticipated then that the stress dependence for an isolated crack in a single crystal of quartz will be much stronger than for brittle rocks. An examination of the published results on creep in brittle rocks does not contradict this view. For example, Rummel's (1968) data on granite at 24°C suggests that the average strain-rate to a strain of 5×10^{-4} increases by a factor of 10^2 for an increase in stress of 230 bars. By way of comparison, the same increase in stress caused an isolated crack to augment its growth rate by a factor of 10^3 . Similar comparisons of the creep results reported by Matsushima (1960b) on granite, Lomnitz (1956) on granodiorite and Misra and Murrel (1965) on granodiorite and gabbro show weaker stress dependencies than that reported here for quartz.

In all cases however, the strain-rate increased exponentially with stress. Tests on granite (Matsushima, 1960b; Rummel, 1968) indicate that the time required for similar samples to exhibit identical creep strains decreases exponentially with stress. A similar analysis at the lateral creep strains also indicates an exponential stress dependence. An exponential stress dependence has been observed for eclogite (Rummel, 1968), micro-granodiorite (Misra and Murrel, 1965), granodiorite and gabbro (Lomnitz, 1956), Lomnitz made his creep measurements in torsion whereas all the others were in compression.

It appears therefore that while the stress dependence for the creep of brittle rocks is exponential in form, the dependence is less pronounced than that observed for time-dependent crack growth on single cracks. It is likely that the stress dependence of rocks in creep depends on many factors such as initial crack density, grain size, mineralogy and the degree of weathering in the mineral grains. If the only effect of increasing stress

was to augment the rate of crack growth on pre-existing cracks then the stress dependence for an isolated crack in quartz should closely approximate that in rocks, especially quartzites. Obviously the situation is not that simple, an increase in stress opens new cracks and causes some pre-existing cracks to grow rapidly to grain boundaries where they may cease growing. Such competing effects tend to complicate any simple, straightforward approach to the stress dependence of rocks in creep. Furthermore most crystalline rocks are made up of silicates that have good cleavage. Axial cracks along such cleavage planes may not undergo the same time-dependent growth as cracks along non-cleavage planes. In light of these difficulties it seems that more creep measurements, especially on quartzite are required. Such data would be extremely useful in comparing the magnitudes of the stress-dependence of quartzite in creep and time-dependent crack growth on single cracks.

The question now arises as to the relation of the temperature and partial pressure of water dependencies between crack growth and creep in rocks. Using an analysis similar to that employed above, if the effect water and temperature on the creep of rocks is to be the same as for crack growth, then the only effect due to an increase in temperature or water content should be to increase the rate of crack growth on pre-existing cracks. An increase in either the temperature or partial pressure of water may have the same effect as increasing the stress and will be subject to the difficulties discussed above. In that case one would expect the activation energy for creep to be only of the same order as that for crack growth but not identical. Similarly, the effect of water content on creep should only obey the same form as that for crack growth and need not

necessarily be identical to establish time-dependent crack growth as the primary mechanism of time-dependent deformation in rocks.

Unfortunately no work has been done on the effect of small variations in water content on the creep of brittle rocks. Some data does exist though for the effect of temperature on the creep in brittle rocks. While Misra and Murrell (1965) and Rummel (1968) measured creep on brittle rocks at room pressure as a function of temperature, their results are suspect. By increasing the temperature, the amount of thermal cracking also increased. Since all the samples were not all heated to a temperature at least as high as the highest test temperature, the initial crack density on each sample was not similar. Because creep is in some way dependent on the initial crack distribution within the sample, the results on the temperature dependence they report must be viewed with caution. In effect then, by increasing the temperature the material properties changed to the extent that a different material was being tested at each temperature. Due to this it is not possible to determine a single activation energy over the temperatures reported from the data presented by Misra and Murrell (1965) and Rummel (1968). For example, Rummel conducted tests on granite load in uniaxial compression to 870 bars at 24°C, 200°C and 400°C. The activation energy was computed in the same manner as the activation energy for crack growth. The ratios of the times required for a rock to achieve an axial strain of 2×10^{-4} was plotted against $1/T^{\circ}K$. The activation energy for the 200° to 400°C range was 10.2 kcal/mole while the analysis between 24°C and 200°C yields a value of 2.9 kcal/mole. This result can be interpreted either as a consequence of thermal cracking or as a change in the mechanism of creep. In light of the fact that dilatancy is observed even at 400°C,

thermal cracking is the most likely explanation.

It appears then that the existing data on creep is not sufficient to make a strong analytical case for time-dependent crack growth as the primary mechanism for creep in brittle crystalline rocks. Obviously more creep data, especially on quartzite, is needed to make significant comparisons between time-dependent crack growth and the creep of brittle rocks. In spite of this shortcoming the composite evidence strongly suggests that time-dependent crack growth is the dominant mode of deformation in creep. Although the stress-dependencies on creep are not as strong as for crack growth, they at least are of the same form and the form of the time-dependent deformation during creep is the same as for time-dependent crack growth. Therefore while the existing data is limited, it in no way is inconsistent with a creep mechanism of time-dependent crack growth and all the evidence points in that direction.

In order to make additional comparisons between crack growth and creep in brittle rocks much more data is required especially on quartzite. The most pressing need is for creep experiments at atmospheric pressure and low confining pressures as a function of temperature and stress. Every effort must be made that thermal cracking is reduced to a minimum to make these tests meaningful. Furthermore, it would be of interest to examine the partial pressure of water dependence on creep and compare it with the results obtained for crack growth. It may be difficult to examine the partial pressure of water dependence on creep in brittle rocks with the same certainty reported for isolated cracks in single crystals. This is due to the inability to insure that every crack and pore in the rock is at the same initial partial pressure of water and that this value corresponds to that in the atmosphere surrounding the sample.

CREEP THRESHOLD

Several questions with respect to creep remain unanswered. First, if crack growth is responsible for creep, is there a creep threshold below which no creep occurs? How is the phenomenon of creep recovery observed by Lomnitz in granodiorite and gabbro related to crack growth, if at all? Finally, is steady-state creep a real feature of creep of brittle crystalline rocks or is it a reflection of the duration of the test?

Any discussion of the concept of a creep threshold requires further clarification. First, is there a lower limit for axial cracking? Second, are there other time-dependent brittle processes that can produce creep at stress levels below those required for axial crack growth? The lower limit for axial crack growth will not be a unique point but will depend on temperature, stress and partial pressure of water at the crack tip. However, at a given temperature and partial pressure of water, the threshold of crack growth will be determined by the stress necessary to produce sufficient energy to drive the hydration reaction between the Si-O bonds. In terms of equation (13) this means that

$$\ln \frac{v}{v_0} = n \ln p_A - \left\{ \Delta F - V^* \sigma + \frac{V_m^* \sigma}{r} \right\} / RT \quad (23)$$

must equal unity, and then the rate of the reaction at the crack tip will equal zero. Since the exact values for equation (13) are not those obtained in this study it is difficult to calculate the threshold for creep directly. In order to compute such a threshold additional work on the reactions between silicates and small concentrations of water is necessary.

It is possible to explain creep at lower stress levels, prior to the

initiation of axial crack growth on a large scale, by considering the possibility of time-dependent sliding between grains. Byerlee (1967) proposed a theory of friction based on the brittle fracture of interlocking asperities between the sliding surfaces. These asperities may undergo time-dependent fracture, as in static fatigue. The rate of slippage between the two surfaces will be a function of the rate of environment-sensitive failure of the asperities. The time-dependent strain of the rock will be proportional to the number of grain boundaries and cracks that undergo sliding. Therefore, to assign a creep threshold is difficult, especially since two types of time-dependent phenomena may occur depending on the stress level. Furthermore, since grain boundary sliding occurs at low stress levels, creep may occur as soon as there is sufficient stress for grain boundary sliding commence. Finally, a distinction between creep due to axial crack growth and grain boundary sliding must be made. It is unlikely that rock failure will occur due to grain boundary creep alone. All the experimental results indicate that brittle failure is accompanied by axial cracking.

The recovery observed by Lomnitz on granodiorite and gabbro may also be due to time-dependent grain boundary sliding. Walsh (1965) described the hysteresis observed in unloading a rock in terms of the frictional sliding on closed cracks. In a rock these closed cracks probably exist at inclined grain boundaries. When the rock is unloaded, isolated axial cracks will close immediately. However, axial cracks which form at the ends of inclined cracks may not close as suddenly. Due to slight rearrangements between grains, the surfaces will not be able to return to their initial position and stresses will be "locked" in the rock. Time-dependent sliding

between these surfaces, due to static fatigue of the asperities on the surfaces, will permit the axial cracks to close in time, and strain to decrease. Hence, recovery is also an environment-sensitive brittle phenomena.

If axial crack growth is the primary mechanism of creep in brittle crystalline rocks and the rate of crack growth is proportional to the rate of strain of the rock, the concept of a truly steady-state creep in such rocks is difficult to imagine. Axial cracks in quartz exhibited a constantly decreasing rate of crack growth. This is due to the fact that the rate at which water was supplied to the crack tip constantly decreased due to a reduction in the free energy of the system and an increase in the path length for diffusion as the crack front advanced. If the mechanism of crack growth in rocks is similar to that in isolated axial cracks, then it is unlikely that a truly steady-state situation will ever be reached. Over intervals on the order of one day, or longer if cracks are extremely short, it may be possible to make an empirical case for a steady-state region. However, since steady-state would imply the rate at which water is supplied to the crack tip is constant secondary creep is a more appropriate term to describe this region.

STRAIN-RATE DEPENDENCE ON THE STRENGTH OF BRITTLE ROCKS

The effect of strain-rate on the strength of brittle crystalline rocks in compression at low confining pressures has been reported by Green and Perkins (1968) and Brace and Martin (1968). As the strain rate decreases there is a corresponding decrease in strength and also in the stress required

to produce a given axial or lateral strain. Since the dilatancy in brittle rocks under compression is related to the opening of axial cracks, it is not improbable that the observed strain-rate dependency can be interpreted in terms of time-dependent axial crack growth. If the observed strain, in a rock is related only to the crack length in each region it is possible to describe a simple sequence of events in terms of time-dependent cracking that yields a strain-rate dependence. In a constant strain or stress-rate test the increase in applied stress is proportional to time. An average stress-rate can also be achieved by increasing the stress by a constant amount at set time intervals. As the time interval increases the average stress-rate decreases. Consider the behavior of a crack in such an experiment. As the load is applied, the crack extends and will continue to extend at a rate determined by the local stress until that stress is increased by increasing the applied load. For each incremental increase in load, the rate of crack growth will increase. As the time interval is increased and the average stress-rate decreased, the distance a crack extends in each interval increases and the total number of stress increments required to produce a desired crack length decreases relative to a similar sample experiencing the same stress increments but at shorter time intervals. Hence, the total stress required to extend a crack to any length decreases with decreasing stress-rate and since the strain is proportional in some way to the crack length the stress required to produce any strain should also decrease with a decrease in stress-rate.

Moreover, the decrease in strength with an increase in moisture content (Charles, 1959; Krokosky and Husak, 1968) can be explained in a similar way. In this case, however, it is not necessary to increase the time

interval at each stress level to allow for a relative increase in crack length. Merely by increasing the partial pressure of water in the crack, the distance a crack extends in each time interval increases and the total number of stress increments necessary to achieve a given crack length decreases relative to a similar sample with a lower partial pressure of water in the cracks. Therefore, the effect of decreasing strength with increasing moisture content is consistent with environment-sensitive crack growth.

GEOLOGICAL APPLICATIONS

PRESENCE OF WATER IN THE CRUST

Up to this point the discussion of crack growth and its role in the time-dependent deformation of brittle rocks has been devoid of any direct geological significance. It might be asked then, in what way the effects presented in this work are applicable to the earth.

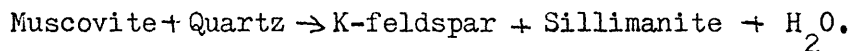
Most crystalline silicate rocks typical of the upper crust, say the top 10 km or so, have exhibited brittle behavior in laboratory tests to several hundred degrees centigrade. Furthermore, temperatures and pressures in the upper crust probably do not exceed 400°C and 4 kb respectively and thus, the rocks through much of the region are still within the brittle regime. Since one major result in this study is that small changes in the partial pressure of water significantly affect the rate of crack growth in a brittle material undergoing deformation, it is necessary to demonstrate the existence of water in the crust before any significance can be attached to the role of environment sensitive crack growth in the earth.

Ample evidence exists for the presence of water in the crust. First, there have been direct measurements of water pressure at the base of deep wells. For example, at the base of the 4 km deep Rocky Mountain Arsenal Waste Disposal Well, near Denver, Colorado, the water pore pressure prior to fluid injection has been reported as approximately 275 bars (Healy et. al., 1968). In addition to direct measurements at well bottoms a wide range of field and laboratory studies point to the presence of water throughout the upper crust, especially in tectonic zones.

It is not unlikely that sediments deposited in shallow marine environments and subsequently buried maintain some of their interstitial water.

For example, the Appalachian geosyncline persisted in the eastern United States through almost all of Paleozoic time. During most of this period shallow marine sediments accumulated in the eugeosyncline and reached thicknesses of 12 km in some regions. The fact that all the sediments are characteristic of a shallow marine environment suggests that the trough was continually subsiding under the weight of the accumulating sediment. Hence, water, trapped in the sediment, subsided with the sediment into the upper crust. Sediments that have accumulated in other geosyncline belts throughout the world also are characteristically shallow marine. Therefore, at least in active orogenic belts, it seems likely that water is present in the upper crust.

Furthermore, laboratory experiments on the stability fields of hydrous silicate minerals suggest values for the partial pressure of water in the earth during the formation of various mineral assemblages. Wones and Eugster (1965) studied biotite stability. Based on these results they concluded that the regional metamorphism of the northwest Adirondaks occurred between 500 and 600°C with a water fugacity between 0.1 and 10 bars. Richardson et.al. (1968) proposed a much higher water fugacity for the equilibrium reaction



For this reaction at 600°C, their results suggest that a fugacity of water of 1270 bars is required. Although the magnitudes of the partial pressures of water required for the formation of hydrous minerals at a given temperature vary widely depending on the mineral assemblages considered, the fact that these hydrous minerals form at all is strong evidence for the existence of water in the earth's crust.

If water is present in the crust then, and environment sensitive crack growth can occur, it might be asked how this effect contributes to large scale geological processes going on in the earth. Several possible implications of time-dependent cracking are outlined below.

FAULT CREEP AND AFTERSHOCKS

Time-dependent fault slippage is a feature well-suited to analysis in terms of brittle behavior. Studies of fault creep on the San Andreas fault show that the slip is both seismic and aseismic (Smith and Wyss, 1968). That is, displacement between the fault surfaces can be accomplished suddenly, accompanied by a sudden stress drop, or gradually with no detectable seismic energy released. This situation may be similar to what is observed in laboratory experiments on natural faults and saw cuts. Frictional sliding experiments show that the relative motion between the surfaces is intermittent and accompanied by sizeable stress drops (Byerlee, 1967; Brace and Byerlee, 1966, 1970). This intermittent motion, called stick-slip, has been proposed as a mechanism for earthquakes. However, not all the motion between the surfaces is characterized by stick-slip. Stable sliding, which is a continuous increase in displacement with no stress drop, was also observed. Presumably stable sliding corresponds to fault creep.

Scholz (1968a) studied the microfracturing associated with stable sliding and stick slip and found that microfracturing was associated with frictional sliding regardless of the sliding regime. Therefore, frictional sliding is a brittle phenomena due to the brittle fracture of asperities on or near the frictional surfaces. Based on these observations Scholz

(1968b) proposed that aftershocks and fault creep are both due to time-dependent brittle fracture in regions of high stress concentration produced by a large earthquake. Scholz reasoned that if the aftershock sequence and fault creep occur independently, then both should decay exponentially with time. This is in agreement with the effect of stress on the time-dependent crack growth in quartz. For a random distribution of stresses, acting on independent regions, the static fatigue failure will be in direct proportion to the stress-dependence on the rate of crack growth. Since the time for a crack to extend to a critical length decreases exponentially with decreasing stress, the number of aftershocks should also decrease exponentially with time. Smith and Wyss (1968) observed that aftershocks along the San Andreas decrease exponentially with time. Furthermore, the cumulative fault displacement due to fault creep also decreased exponentially with time.

Fault creep however, was not continuous but episodic. Based on these observations Scholz et.al. (1969) concluded that fault creep and aftershock sequences are identical processes acting independently but in one case time-dependent failure leads to macroscopic fracture and in the other smooth slip. Both then are related to stress concentrations produced by the main shock, but are not interrelated.

It appears then that brittle failure due to time-dependent crack growth is capable of producing a consistent explanation of fault creep and fore-shock and aftershock sequences. Further studies on frictional sliding (Byerlee and Brace, 1968) showed stick slip is a function of rock type and confining pressure. For example, stick slip occurred in Westerly granite on both natural faults and saw cuts above confining^{pressure} of approximately one kilobar, while Spruce Pine dunite exhibited stable sliding at all confining

pressures examined. It was found that those rock types that showed ductile behavior at all confining pressures generally contained either alteration products, such as serpentine, or calcite. Based on these observations rocks such as Westerly granite, San Marcos gabbro, and Dedham granodiorite which were characterized by stick slip above one kilobar confining pressure were termed Type I rocks, while such rocks as Spruce Pine dunite and Solenhofen limestone which exhibited stable sliding were termed Type II. In light of these results, Byerlee and Brace suggest that the relation between rock type and stick slip and stable sliding may explain earthquakes and fault creep. Presumably the spacial distribution of rock types will determine the nature of fault activity in a given region.

STICK SLIP AND STABLE SLIDING AS A FUNCTION OF TIME-DEPENDENT CRACK GROWTH

While these arguments satisfactorily explain the field of observations, several questions remain unanswered with respect to stick slip and stable sliding in laboratory experiments. First, on a microscopic level, what is the fundamental difference between stick slip and stable sliding? Is there a transition from stick slip to stable sliding as a function of strain-rate, temperature and partial pressure of water? If such a transition exists, can it be attributed to time-dependent crack growth? Since Scholz (1960a) observed micro-fracturing, it is worthwhile to examine the role of time-dependent crack growth in frictional sliding as well as other brittle phenomena. Furthermore, because the reason for undertaking this study was to assess the effect of crack growth in brittle rocks, let us examine some of the effects observed in Type I rocks with the emphasis on what will

happen as a function of time. The behavior of Type II rocks which presumably will exhibit a behavior which is in part due to crack growth and in part due to the percentage and properties of the alteration products, will not be considered. The approach then will be to examine some of the effects observed on typical brittle rocks both in fracture and frictional sliding tests to ascertain any common characteristics which may enhance our understanding of the transition between stick-slip and stable sliding.

The dependence of the compressive strength on the strain-rate of water saturated Westerly granite, at a confining pressure of 1.56 kb over a range of 2.4×10^{-3} to $2.4 \times 10^{-7} \text{ sec}^{-1}$, has been reported as a decrease of 10 per cent per three decades (Brace and Martin, 1968). In all these experiments, the samples failed suddenly, with an audible stress drop, along a shear fracture at approximately 30° to the maximum compressive stress. A question must be answered prior to extrapolating these results to the earth. Will the granite continue to fail catastrophically at geological strain-rates? It is possible to examine the problem of sudden, audible stress drops at failure. Let us consider the failure of Westerly granite with an increase in the partial pressure of water. Brace and Martin (1968) studied the effect of pore pressure on the strength of Westerly at an effective confining pressure of 1.56 kb at strain-rates from 10^{-3} to 10^{-7} sec^{-1} . While all the saturated samples at a confining pressure of 1.56 kb failed suddenly with an audible stress drop, samples with a confining pressure 3.12 kb and a pore pressure of 1.56 kb did not always fail audibly. At strain-rates greater than 10^{-6} sec^{-1} , the samples failed with an audible stress drop; the fracture strength however was greater than that for saturated samples at the same strain-rate. This strengthening was attributed to dilatancy hardening; as the porosity increased during

deformation, the pore pressure dropped, the effective confining pressure increased, and the rock appeared stronger. At strain-rates of 10^{-6} and 10^{-7} however the samples failed without audible stress drops at fracture strengths nearly equal to saturated samples tested at the same strain-rate. It was concluded that the strain-rate at which the saturated sample and the sample with pore pressure became equal was the critical strain-rate for the validity of the effective stress law.

When the samples were examined, there was no obvious difference in the nature of faulting between the saturated samples and those tested with pore pressure. A sample of Westerly granite tested at 10^{-7} sec^{-1} with pore pressure was embedded in Stycast and a polished section examined (Martin, 1968). The Stycast impregnated the sample along the fault zone which appeared as a broad region several millimeters wide on either side of the fault plane. There was no evidence of impregnation along the boundary of the sample. Samples of the same granite tested at a confining pressure of 1 kb at strain-rates on the order of 10^{-5} sec^{-1} showed no tendency for impregnation into regions adjacent to the fault when they were imbedded in Stycast.

What does this observation mean in terms of crack growth? It appears that the large increase in porosity prior to failure is spread over a broader zone with pore pressure than without at the same strain-rate. Since the partial pressure of water, in the form of pore pressure, increases the rate of crack growth, cracks, throughout the rock as well as in the fault zone, extend stably to greater lengths at lower stress levels, and time-dependent crack growth increases in significance relative to the effect of augmenting the stress. Hence, as the stress is increased there is not

as much of a tendency for an instability to become localized and result in a sudden failure. This suggests that the critical strain-rate reported by Brace and Martin is not solely determined by the rate at which the pore pressure builds up in a sample after an increment of dilatancy but is also a function of the effect of the partial pressure of water on crack growth. If this is true, then the pore pressure is not fully recovered at a strain rate of 10^{-7} sec^{-1} and at lower strain-rates the strength should be less than a saturated sample tested at the same strain-rate. Unfortunately, the tests on Westerly granite were not extended below 10^{-7} sec^{-1} . One sample of Maryland diabase was run at 10^{-8} sec^{-1} however, and the strength was lower than what would be expected for a saturated rock tested at the same effective confining pressure and strain-rate.

If this transition from sudden audible stress drops at failure to inaudible failure with gradual stress drops is related to time-dependent crack growth, then saturated samples should undergo the same transition at lower strain-rates. Based on the fact that an increase in partial pressure of water of approximately 10^3 increases the rate of crack growth by nearly 10^3 , one would expect the same transition to occur at a strain-rate of 10^{-9} to $10^{-10} \text{ sec}^{-1}$.

Unfortunately the strain-rates are too low to test this prediction in the laboratory. However, since an increase in temperature has the same effect as increasing the partial pressure of water, the same transition from audible to inaudible failure observed with a pore pressure of 1.56 kb at room temperature should occur in a saturated sample at a confining pressure of 1.56 kb in the vicinity of 150°C at the same strain-rate. Although the transition has not been studied per se, all the existing data is consistent with the time-dependent crack growth interpretation. Byerlee (1967) reported that Westerly granite failed violently at all confining

pressures at room temperature. Griggs et al. (1960) found that Westerly granite tested at 300°C and 5 kb confining pressure failed in shear but without an audible stress drop. While these results are all in the correct direction if the transition is related to time-dependent crack growth, further studies of this effect as a function of strain-rate, temperature, and pore pressure, as well as confining pressure are necessary to define the boundaries between regions of violent and gradual failure.

Finally, since cracking is believed to be associated with frictional sliding it seems reasonable to ask what effect time-dependent crack growth should have on the transition from stick slip to stable sliding. If the mechanism of frictional sliding is primarily due to fracture of interlocking brittle asperities (Byerlee, 1967b) and fracturing is accomplished by crack growth, then it would be expected that frictional strength will be dependent on temperature, pore pressure, and strain rate. Byerlee and Brace (1968) measured the frictional strength of Westerly granite as a function of strain rate. Over a range of strain-rates from 2.4×10^{-4} to 2.4×10^{-6} sec⁻¹ and 4.25 kb confining pressure, no decrease in frictional strength was observed with a decrease in strain-rate. Perhaps the confining pressure was too high to observe any effect over the range of strain-rates examined, since the data presented indicates that there is also no decrease in fracture stress with decreasing strain-rate such as observed by Brace and Martin, (1968) at 1.56 kb. However, a decrease in frictional strength with increased temperature was observed (Brace and Byerlee, 1970). This is consistent with the temperature effect on crack growth since cracks will attain the same length at lower stresses with an increase in temperature. It is possible therefore that a time-dependent frictional strength exists

but the effect is not large over laboratory strain-rates especially at high confining pressures.

This leads to the problem of stick slip versus stable sliding. Is it possible that this transition is related to time-dependent crack growth in the same manner as the transition from sudden to gradual failure in compression tests? At high strain-rates and low temperatures, cracking is dominated by the rate of increase in stress. Presumably this leads to a localized instability and sudden slippage. Consider another test at the same strain-rate and confining pressure, but at a high temperature or pore pressure. More crack growth will take place at lower stress levels and the ultimate failure distributed over a wider region. This non-localized failure on the surfaces may produce gradual instead of jerky slip. Brace and Byerlee (1970) measured frictional sliding as a function of confining pressure and temperature. For Westerly granite, they found that as the confining pressure and temperature were increased stick slip gave way to stable sliding. At strain-rates of 10^{-4} to 10^{-6} sec^{-1} the transition from one mode to the other was nearly equal to the geothermal gradient. No strain-rate dependence was observed over this range. Therefore, if the transition from stick slip to stable sliding is due to time-dependent crack growth, further experiments at lower confining pressures, similar to those used by Brace and Martin (1968), may be required to test this possibility experimentally.

FRACTURING ASSOCIATED WITH IGNEOUS ACTIVITY

The importance of water on the rate of crack growth leading to the fracture of rocks is not restricted to earthquake related problems. Water

may facilitate the formation of many of the observed features associated with the intrusion of plutons.

One of the most striking features associated with the intrusion of some plutonic bodies is the formation of ring-dikes and cone sheets. These discordant igneous features have been attributed to the forceful injection of magmatic material into fractures that formed due to the differential stress generated by the magma pushing on its surrounding walls (Anderson, 1951). Near the surface, field data indicates that the magma does not melt the surrounding country rock but is discordantly implaced in it and thus the country rock will remain in the brittle regime, that is, if it is a typical crystalline silicate.

This presents an interesting situation. Since water exists in magma chambers, it more than likely facilitated the growth of cracks which lead to the formation of the fractures now occupied by the dikes and cone sheets. The question here then is not so much, "How do small variations in the amount of water influence the rate of formation of ring dikes and cone sheets?" but rather "In a situation where there is no water, will such features form at all?" As we have shown, the rate of crack growth decreases with decreasing partial pressure of water, and for exceedingly low partial pressures of water, on the order of 10^{-7} to 10^{-10} mb, it may be arrested altogether at stresses generated by the magma. Therefore, for an exceedingly dry magma or on a planet with no water, such features as ring dikes, cone sheets or even radial dike swarms may form, but much higher stresses would be required than for water rich magmas.

The presence of water in the magma chamber and surrounding rocks not only facilitates the formation of fractures extending to the surface but

also may serve to enhance the mobility of a rising magma. Large magmatic bodies move by stoping. The roof of the magma chamber is fractured causing blocks of country rock to subside into the magma where they are preserved as xenoliths. By continually shattering the roof of the magma and assimilating the fractured blocks, the magma rises. This process is called stoping. Once again it is the water in the magma and its vicinity that reduces the strength of the surrounding bedrock thereby facilitating the mobility of magmatic bodies. Therefore, the mobility of magmas and the large scale features related to their emplacement are obviously enhanced by the presence of water as a weakening agent in the brittle fracture of the surrounding country rock.

In addition to the dikes associated with the intrusion of plutons, many dikes are associated with extrusive igneous activity. Often dikes form in the vicinity of volcanoes. These dikes may be no more than remnants of fissures opened by the pressure exerted by a rising magma where water facilitated the opening of the rift.

In conclusion then, water facilitates the formation of brittle fractures in the country rock surrounding igneous plutons. The stress to open the fractures are generated by the magma. Furthermore, it is possible that for dry magmas or on planets devoid of water, that the movement of magmas will be controlled by the melting of the country rock or the hydraulic action of highly viscous magmas not by stoping due to water corrosion enhanced fracture.

CONCLUSIONS

Environment sensitive time-dependent crack growth is a measurable effect in a brittle material. The rate of axial crack growth in single

crystals of quartz loaded in uniaxial compression was observed as a function of stress temperature and partial pressure of water in the atmosphere surrounding the sample. An increase in either the temperature, stress or partial pressure of water increased the rate of crack growth.

The data was analyzed in terms of the time required for a crack to extend an arbitrarily selected increment of 0.20 mm. Experiments were compared by examining the relative time for each crack to extend 0.20 mm as one parameter was varied. For example, by decreasing the temperature from 188°C to 93°C, the relative time required for a crack to extend the 0.20 mm increased by 10^3 . The same effect can also be produced by decreasing the stress 200 bars or decreasing the partial pressure of water by a factor of 10^3 .

The time-dependent crack growth was found to obey a power law of the form $C = At^n$ where A and n are constants. Typically n ranges between 0.2 and 0.8 and increases with an increase in stress, temperature or partial pressure of water. An analysis of the data in terms of the relative times for a crack to extend 0.20 mm as one parameter was varied showed that the temperature dependence could be expressed in terms of a activation energy of 25.8 ± 0.6 kcal/mole. The rate of crack growth increased exponentially with increasing stress and increased as a power law with an exponent of -0.95 with increasing partial pressure of water.

These results are in general agreement with the stress corrosion theory of crack growth proposed by Hillig and Charles (1965). Although stress corrosion theory adequately describes the process of hydrating and rupturing Si-O bonds at the crack tip, the rate of this process is limited by the rate at which water is transported to the crack tip. Hence, the diffusion

rate is the limiting factor in environment sensitive time-dependent crack growth.

Time-dependent crack growth is shown to be consistent with observed strain-rate of brittle rocks tested in creep. Moreover, the stress and temperature dependence observed in creep is of the same form as the stress and temperature dependent of time-dependent crack growth. On this basis it is concluded that time-dependent crack growth is a principle mechanism of creep in brittle rocks below approximately 400°C.

Static fatigue of such brittle materials as glass, crystalline rocks and quartz is also due to time-dependent crack growth. The time to failure increases exponentially with decreasing stress or with decreasing partial pressure of water. This is in agreement with the observations of time-dependent crack growth. Moreover the activation energies obtained on the static fatigue of silicate materials are similar to those reported in this study. This is a further indication that environment sensitive time-dependent crack growth is responsible for the static fatigue of brittle materials.

Finally time-dependent cracking is explored as a mechanism of stable sliding and stick slip. It has been proposed that frictional sliding is due to the brittle fracture of interlocking asperities between the two surfaces. Since brittle fracture is due to crack growth, time-dependent failure of these asperities should lead to time-dependent frictional sliding. Presumably then the transition between stick slip and stable sliding will be a function of the rate of crack growth. Rapid unstable crack growth at low temperatures and high strain-rates may cause stick slip while lower strain-rates and higher temperatures permit cracks to lengthen at lower stress

levels and produce a more randomly distributed failure of asperities, spacially and temporarily and lead to stable sliding.

SUGGESTIONS FOR FUTURE RESEARCH

Several areas of possible interest for future work have been pointed out in the text. Some of these suggestions will be reviewed here.

First, further crack studies of the type reported here should be conducted to establish the relation between the conchoidal nature of the crack surface, the rate of crack growth, and the microfracturing events emitted during crack growth. These results may then be compared with the microfracturing observed on quartz in static fatigue and on brittle rocks during creep.

Since only a limited amount of data exists on creep in brittle rocks, it would be of interest to conduct additional tests to (i) establish a creep threshold, (ii) see if the activation energies for creep are similar to those for time-dependent crack growth, (iii) determine whether or not the moisture dependence observed for environment sensitive time-dependent crack growth can be demonstrated for creep in brittle rocks, (iv) measure the frequency of microfracturing during creep and relate it to any microfracturing observed in crack growth and (v) estimate the maximum temperature and confining pressure at which crack growth is the principal mechanism of creep.

Additional studies on frictional sliding should be conducted over a wide range of strain-rates, say from 10^{-7} to 10^{-3} sec^{-1} at low confining pressures, to determine if the transition from stick slip to stable sliding is strain-

rate sensitive. Furthermore to determine whether or not crack growth is a prominent mechanism in frictional sliding over a wide temperature range microfracturing events should be recorded to establish the extent of cracking as the temperature is increased up to 400 or 500°C.

ACKNOWLEDGEMENTS

I am especially indebted to W.F. Brace for his continued interest and suggestions during the course of this study. In addition J.B. Walsh and C. Goetze made important suggestions. M.L. Smith aided in the data reduction.

I wish also to thank the John A. Lyons Fund for their financial aid during the last two and one half years.

BIBLIOGRAPHY

- Anderson, E.M., The dynamics of faulting and dyke formation with applications to Britain, Oliver and Boyd, London, 1951.
- Bieniawski, Z.T., Stability concept of brittle fracture propagation in rocks, Eng. Geol., 2, 149, 1967.
- Brace, W.F., and E.G. Bombolakis, A note on brittle crack growth in compression, J. Geophys. Res., 68 (12), 1963.
- Brace, W.F., and J.D. Byerlee, California earthquakes: Why only shallow focus?, Science, 168, 1573, 1970.
- Brace, W.F., and R.J. Martin, III A test of the law of effective stress for low porosity crystalline rocks, Int. J. Rock Mech. Min. Sci., 5 415, 1968.
- Brace, W.F., A.S. Orange and T.M. Madden, The effect of pressure on the electrical resistivity of water-saturated crystalline rocks, J. Geophys. Res., 70 (22), 5669, 1965.
- Brace, W.F., B.W. Paulding, Jr., and C.H. Scholz, Dilatancy in the fracture of crystalline rocks, J. Geophys. Res., 71 (16), 3939-3953, (1966).
- Brace, W.F., and D.K. Riley, Uniaxial strain behavior of fifteen rocks to 30 kb, Trans. Am. Geophys. Union, 52 (4), 346, 1971.
- Brophy, J.H., R.M. Rose and J. Wulff, Thermodynamics of structure, Structure and Properties of Materials, Vol. 2, 1964.
- Byerlee, James D., Theory of friction based on brittle fracture, J. Appl. Phys., 38 (7), 2928, 1967.
- Byerlee, J.B., and W.F. Brace, Stick-slip, stable sliding and earthquakes - effect of rock type, pressure, strain rate and stiffness, J. Geophys. Res., 73 (18), 6031, 1968.
- Byerlee, J.D., and W.F. Brace, High pressure mechanical instability in rocks, Science, 164, 713, 1969.
- Charles, R.J., The strength of silicate glasses and some crystalline oxides, in Proceedings of the International Conference on Fracture, pp. 225-250, M.I.T. Press, Cambridge, Mass., 1959.
- Goetze, Christopher, High temperature rheology of Westerly granite, J. Geophys. Res., 76 (5), 1223, 1971.
- Green, S.J., and R.D. Perkins, Uniaxial Compression tests at strain rates from 10^{-4} to 10^4 /sec. on three geologic materials, Proceedings of the Tenth Symposium on Rock Mechanics, (1968).

- Griggs, D.T., F.J. Turner and H.C. Heard, Deformation of Rocks at 500°C to 800°C, GSA Mem. 79, 39-104, 1960.
- Healy, J.H., W.W. Rubey, D.T. Griggs, and C.B. Raleigh, The Denver earthquakes, Science, 161 (3848), 1301, 1968.
- Heard, H.C. Experimental deformation of rocks and the problem of extrapolation to nature, N.S.F. Advanced science seminar in rock mechanics, V.2, R.E. Reicher, ed., 1968.
- Heard, H.C., and N.L. Carter, Experimentally induced "natural" intragranular flow in quartz and quartzite, Am. J. of Science, 266, 1968.
- Hillig, W.B. and R.J. Charles, Surfaces, Stress-dependent surface reactions, and strength, High Strength Materials, John Wiley & Sons, N.Y., 1965.
- Hoek, E., and Z.T. Bieniawski, Brittle fracture propagation in rock under compression, Intl J. Fracture Mechanics, 1 (3), 1965.
- Koide, H., and K. Hoshino, The development of microfractures in experimentally deformed rocks.
- Krokosky, Edward M., and Alan Husak, Strength Characteristics of Basalt Rock in Ultra-High Vacuum, J. Geophys. Res., 73 (6), 2237, 1968.
- LeRoux, Haydeem The strength of fused quartz in water vapor, Proc. Royal Soc. London, A, 286, 390, 1965.
- Martin, R.J., The effect of pore pressure on the strength of low porosity crystalline rocks, M.S. thesis, Massachusetts Institute of Technology, 1967.
- Matsushima, S., Variation in elastic wave velocities of rocks in the deformation and fracture under high pressure, Disaster Prevention Res. Inst., Kyoto Univ., Bull. 32, 1960a.
- Matsushima, S., On the flow and fracture of igneous rocks, Disaster Preventions Res. Inst. Kyoto Univ. Bull., 36, 2, 1960b.
- Peng, Syh-Deng, Fracture and failure of Chelmsford granite, Ph.D. thesis, Stanford University, 1970.
- Richardson, S.W., P.M. Bell and M.C. Gilbert, Kyanite-sillimanite equilibrium between 700°C and 1500°C; Am. J. Sci., 266, 513, 1968.
- Robertson, E.C., Creep of Solenhofen limestone under moderate hydrostatic pressure, Geol. Soc. Am. Memoir 79, 227-244, 1960.
- Rummel, F., Studies of time-dependent deformation of some granite and eclogite samples under uniaxial, constant compressive stress and temperatures up to 400°C, Zeitschrift fur Geophysik, 1969.

- Serdengecti, S. and G.D. Boozer, The effects of strain rate and temperature on the behavior of rocks subjected to triaxial compression, Proceedings of the Fourth Symposium on Rock Mechanics, Pennsylvania State University, pp. 83-97, (1961).
- Scholz, C.H., Microfracturing and the inelastic deformation of rock in compression, J. Geophys. Res., 73 (4), 1968a.
- Scholz, C.H., Mechanism of creep in brittle rock, J. Geophys. Res., 73 (10), 3295-3302, 1968b.
- Scholz, C.H., M. Wyss, and S.W. Smith, Seismic and aseismic slip on the San Andreas fault, J. Geophys. Res., 74 (8), 2049, 1969.
- Scholz, C.H., Static fatigue of quartz, Trans. Am. Geophys. Union, 51(11), 827, 1970.
- Smith, Stewart W., and Max Wyss, Displacement of the San Andreas fault initiated by the 1966 Parkfield earthquake, Bull. Seismol. Soc. Am., 58, 1955, 1968.
- Tocher, Don, Anisotropy in rocks under simple compression, Trans. Am. Geophys. Union, 38, 1957.
- Walsh, J.B., The effect of cracks on the compressibility of rock, J. Geophys. Res., 70 (2), 381-389, 1965.
- Wawersik, Wolfgang R., Detailed analysis of rock failure in laboratory compression tests, Ph.D. thesis, Univ. of Minnesota, 1968.
- Wawersik, W.R., and W.F. Brace, Post failure behavior of a granite and diabase, Tectonophysics, in press, 1971.
- Wiederhorn, S.M., Moisture assisted crack growth in ceramics, Int. J. of Fract. Mech., 4 (2), 171-177, 1968.
- Wiederhorn, S.M., Fracture of ceramics, in Mechanical and Thermal Properties of Ceramics, NBS Spec. Pub. 303, 1969.
- Wones, D.R., and H.P. Eugster, Stability of biotite: Experiment, theory and application, Am. Miner., 50, 1228, 1965.

APPENDIX I

MEASUREMENT OF THE RATE OF CRACK GROWTH

When the study of environment-sensitive crack growth was initiated, it was anticipated that the rate of crack growth could be satisfactorily measured electrically with a crack propagation gage. Crack propagation gages are similar to ordinary strain gages in that they are made up of Nichrome V or constantan strands approximately 0.00015 inches thick, except that the individual strands which make up the gage are connected in parallel instead of in series. The gage is bonded to the sample with the strands normal to the direction of the advancing crack front. As the crack grows, individual elements of the gage fracture near the crack tip, producing an easily monitored change in gage resistance. Since the gage is mounted on the surface of the sample, it is directly influenced by the behavior of the material beneath the gage. Therefore, the correlation between crack position and gage element fracture will depend on the thickness of the epoxy beneath the gage, the amount of tunneling and the magnitude of the total strain in the sample relative to the fracture strain of the gage elements.

The first gage tested was CP-481EX manufactured by the Budd Company. The gage was bonded to the surface of the sample in the same way as a conventional strain gage with the filaments normal to the direction of crack propagation. The gages were backed with phenolic-glass and composed of twenty equally spaced strands over a distance of 0.192 inches. The gage was connected to one arm of a balanced Wheatstone bridge and the output monitored on a strip chart recorder. The filaments on the gage were not all the same length but adjusted so that when each strand was fractured the change in resistance of the gage was nearly the same, and the output on

the strip chart recorder due to fracturing of each element appeared as steps, all nearly the same height.

For the sample size and geometry employed in this study the CP-481EX crack propagation gage proved unsatisfactory. For example, the crack had extended through the entire gage length before any response was observed on the strip chart recorder.

Baldwin, Lima and Hamilton Inc. manufactures a crack propagation gage, called the NASA continuity gage, which is very similar in design and dimensions to the CP-481EX except that it is a free filament gage. Since it was possible that the phenolic-glass backing distributed the strain to such an extent that the filaments did not strain sufficiently to cause rupture, it was felt that this difficulty could be overcome by bonding the filaments directly to the surface of the specimen. Thus, by eliminating the backing on the strain gage, the strain concentration at the crack tip should be transferred directly to the filament and cause rupture.

Although the results with the free filament gage were somewhat more encouraging, the response of the gage still lagged four to five strands behind the crack front. Furthermore, each element of the gage was not ruptured as the crack passed, and continued to change resistance as the crack continued to grow. Consequently, the output was not a series of well defined steps that monitored the position of the crack front as originally anticipated but more of an irregular increase in resistance with the time which could not be correlated with the actual position of the crack tip. Hence, it was concluded that the strain due to an advancing axial crack in quartz was not sufficient to rupture the strands of the commercial crack propagation gages.

In light of these observations it was felt that if a gage could be made thin enough, a one to one correspondence between the location of the crack tip and the gage output could be achieved. One way of achieving a very thin, yet electrically conducting gage, is to evaporate a thin gage of suitable conductor directly on a polished specimen. Gold was selected as the appropriate material to form the active filaments of the gage, because it would not oxidize and change resistance during an experiment in the presence of water. Strips of gold were deposited on the polished sample surface using a BLH FAO-36-125 free filament strain gage as a template. This is the same technique employed to obtain the reference grid for visual observations described in the text. After the strain gage was removed from the sample, the active filaments were connected in parallel using silver conducting epoxy at the ends of the strips. In effect then we were able to produce our own crack propagation gage but with the added advantages of being able to control the thickness of the gage filaments and of eliminating any effects due to the nature of epoxy which bonded the previous two types of gage to the surface.

The gold strips were evaporated on to the samples in the M.I.T. Electron Microscopy Laboratory. During the evaporating process the gold was suspended in a tungsten wire basket directly over the sample. The thickness of the film was controlled by adjusting the height of the basket above the surface of the sample and by varying the mass of gold evaporated. The relation between the mass evaporated in milligrams, M , the film thickness in angstroms, t , and the distance of the basket above the sample in centimeters, r , is given by

$$M = 1.67 \times 10^{-4} tr^2 \rho \quad (1)$$

where ρ is the density of the metal evaporated in g/cm^3 .

Once the thickness of each strand is known and the other dimensions have been measured under a microscope, the theoretical resistance of each filament can be computed using the relation

$$R_s = \eta \frac{l}{wt} \quad (2)$$

where R_s is the resistance of the strand, η is the resistivity of the conductor, l is the length, w is the width and t is the thickness of the strand. If all the elements have the same dimensions then the theoretical resistance of the gage obtained by connecting the strips in parallel is

$$R_G = \frac{R_s}{n} \quad (3)$$

where n is the number of filaments in the gage.

A number of samples were prepared in the manner described above with strand thicknesses ranging from 62 \AA down to 18 \AA . Generally, for thicknesses above 45 \AA , the observed gage resistance agreed within a factor of two with the theoretical gage resistance computed using equations 2 and 3. However, as the thickness of the strands decreased below approximately 45 \AA , the gage resistance began to deviate significantly from the theoretical value often by more than an order of magnitude. The sample with a gage thickness of 18 \AA acted as an open circuit.

The samples were loaded in uniaxial compression in a small hydraulic press and the advancing crack tip was visually correlated with the output from the crack propagation gage. When the gage thickness was greater than 35 \AA or so the response of the gage was very similar to that observed for the BLH NASA continuity gage. That is, the gage response lagged behind

the advancing crack front. For thinner gages, the response was much better. For the most part, the gages behaved well through the first three or four strands of the gage. The output was marked by nearly flat plateaus when the crack tip was between strands and by gradual increase in resistance as the crack propagated through a strand. However, as the crack advanced beyond the first few strands the output became more confusing and the one-to-one correspondence between gage output and crack length broke down. Although these gages were not totally satisfactory for monitoring the time-dependent growth of axial cracks under a constant load, if the stress was continuously increased and the resulting crack growth was governed by the rate of increase in stress, a one-to-one correlation between crack length and gage output was obtained.

Finally, it appeared that the only way to measure time-dependent crack growth electrically was to use a less ductile metal for the active elements in the gage or perfect a gage where the strands were only 10 to 15 Å thick. Since any less ductile metal would be subject to corrosion in the test vessel a thinner gage was attempted. It seemed possible that the cross-sectional area of each strand varied due to the roughness of the surface. Small pits on the surface could cause local thinning in each strand and an increase in strand resistance. Thus if the strand was thin enough or the pits deep enough and closely spaced, the strand may act as an open circuit. Therefore, if the surface of the sample was highly polished, it was felt that workable gages less than 18 Å thick could be obtained. Two samples were polished by World Optics Inc., Waltham, Massachusetts, to the best finish they could achieve. Gages 10 and 15 Å thick, were prepared on these surfaces. Both acted as open circuits.

In light of these difficulties, it was felt that the most precise way to measure time-dependent crack growth was visually, as described in the text. Although meaningful results could be obtained over limited crack lengths with crack propagation gages, extended tests with longer crack lengths or multiple tests on the same sample would be extremely difficult to interpret. Therefore, visual observation eliminated this uncertainty but at the minor expense of constant vigilance.

APPENDIX II

DEPENDENCE OF STRESS CONCENTRATION FACTOR ON CRACK LENGTH

In the analysis of the time-dependent crack growth data, it was stated that the stress concentration factor was not constant with crack length but decreased as the crack extended. This statement was based on the fact that in order to extend the crack several millimeters it was necessary to increase the applied load substantially above that required to initiate the crack. For example, in one of the initial tests to evaluate the crack propagation gages the stress necessary to initiate the crack at the cylindrical hole was 775 bars while the stress required to extend the crack to a length of 5 mm was 1,130 bars. If the crack growth is due to the rupture of bonds at the crack tip and the primary mechanism of propagation is due to the stress at the crack tip then the stress concentration factor decreases with increasing crack length.

It seems appropriate in light of the analysis of the time-dependent crack growth results to ask if the relative magnitude of the stress concentration factor can be estimated. In that way, an estimate of the error due to comparing the results of experiments with slightly different crack lengths can be obtained. An examination of the experimental results produced two experiments well suited to estimate the relative stress concentration factor for crack lengths between 2.57 mm and 3.17 mm. Both experiments were run at 200 °C and 405 mb partial pressure of water, but at different initial crack lengths and applied loads. One sample with an initial crack length of 2.57 mm was tested at 930 bars while the other with an initial crack length of 3.17 mm was tested at 1000 bars. A comparison of the time-dependent crack growth in both experiments showed that the rate

of growth is nearly identical for each test (Figure 15).

In a general way this may indicate that the stress at the crack tip is nearly the same over each increment of crack growth for both experiments. Since the rate of crack growth depends on the partial pressure of water at the crack tip as well as the stress, it is possible that the similar rates of crack growth can also be related in some way to the differences in the rate at which water is transported to the crack tip. In spite of this uncertainty, it seems worthwhile to calculate the relative difference in stress concentration factors between the two experiments assuming that the stress is the same at the tip of each crack at corresponding times.

The stress concentration factor, K , relates the uniform applied stress infinitely removed for the stress raiser, σ_{∞} , to the stress at some inhomogeneity in the material, σ , through the relation

$$K = \frac{\sigma}{\sigma_{\infty}} \quad (1)$$

For example, when a plate with a circular hole is loaded in uniaxial compression, the stress concentration factor at the boundary of the hole 0° and 180° to the direction of the applied stress is -1.

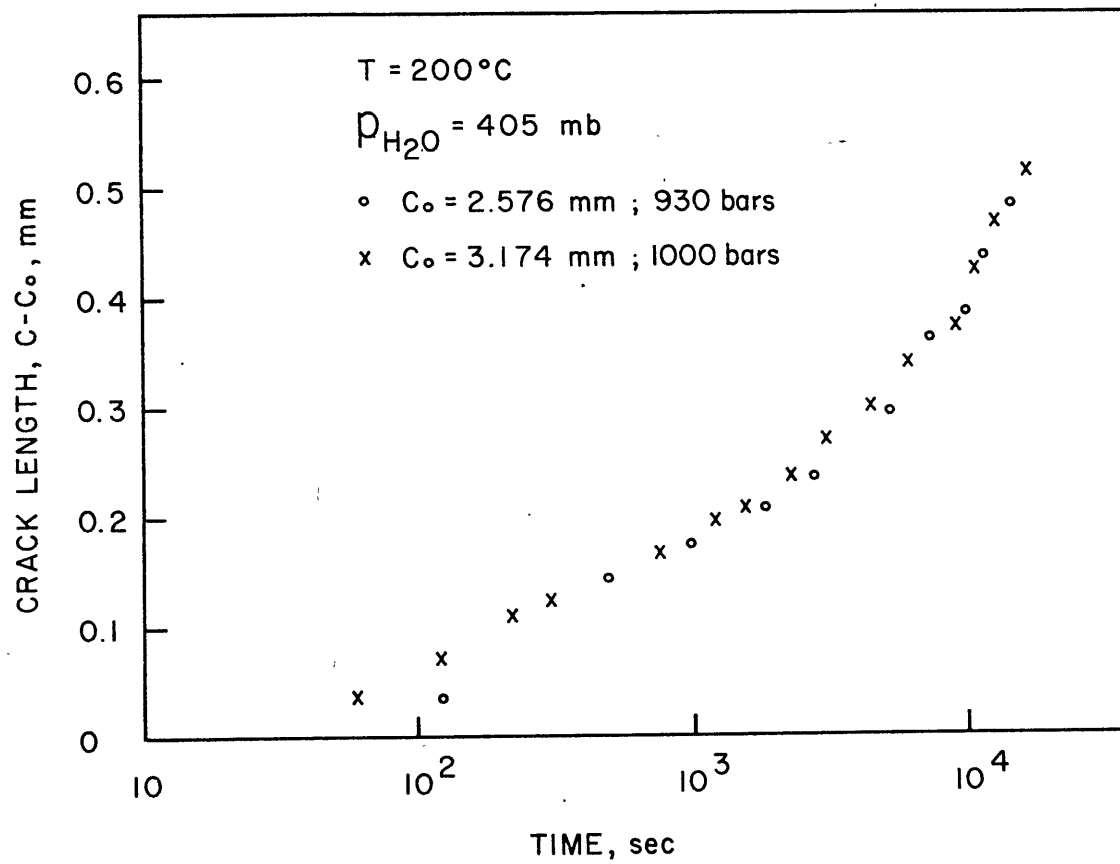
Consider the experimental results in Figure 15. Let us assume that the similarity in the rate of crack growth is primarily due to nearly identical stresses at the crack tip. In that case the stress concentration factor at the crack tip differs in each test. For this condition we can write

$$\sigma = \frac{K_1}{\sigma_1} = \frac{K_2}{\sigma_2} \quad (2)$$

where σ is the stress at the crack tip in both experiments, $\sigma_1 = 1000$ bars and $\sigma_2 = 930$ bars and K_1 and K_2 are the stress concentration factors

Figure 15

Two separate experiments at different stresses and initial crack lengths, but the same temperature and partial pressure of water showing nearly identical rates of time-dependent crack growth.



corresponding to σ_1 and σ_2 at their respective crack lengths. Substituting numerically into equation 2 and solving for the ratio of the stress concentration factors yields 1.08. This means that the stress at the crack tip for an initial crack length of 2.57 mm is 1.08 times that for an initial crack length of 3.17 mm.

Unfortunately only two experiments at the same temperature and partial pressure of water but different stresses and initial crack lengths exhibited identical rates of crack growth. However, it is possible to extend the analysis to longer crack lengths using a similar but somewhat less rigorous approach. Two successive experiments on the same sample were conducted at 655 bars, ~~244~~²⁴⁴°C, and 405 mb partial pressure of water. For the first test the initial crack length was 2.76 mm and for the second 3.77 mm. The rate of crack growth in each experiment was different. In this case, the applied stress is the same but the stress at the crack tip is not. If the difference in stress at the crack tip was known however, the relative stress concentration factors could be estimated. To estimate this difference in stress at the crack tip, let us work backwards from the stress dependence results in Figure 8. The ratio of the times required for these two cracks to extend 0.2 mm was 9. This value corresponds to a decrease in applied stress of 60 bars. This means that for both tests to have identical rates of crack growth the second test should have been conducted at an applied stress 715 bars. Substituting these values into equation 2 and solving for the ratio of the stress concentration factors, a value of 1.08 is obtained. If the stress dependence was computed in terms of the time required for a crack to extend any distance but 0.20 mm, the relative difference in stress concentration factors would vary accordingly. Therefore, this value of 1.08 represents only a general indication of relative

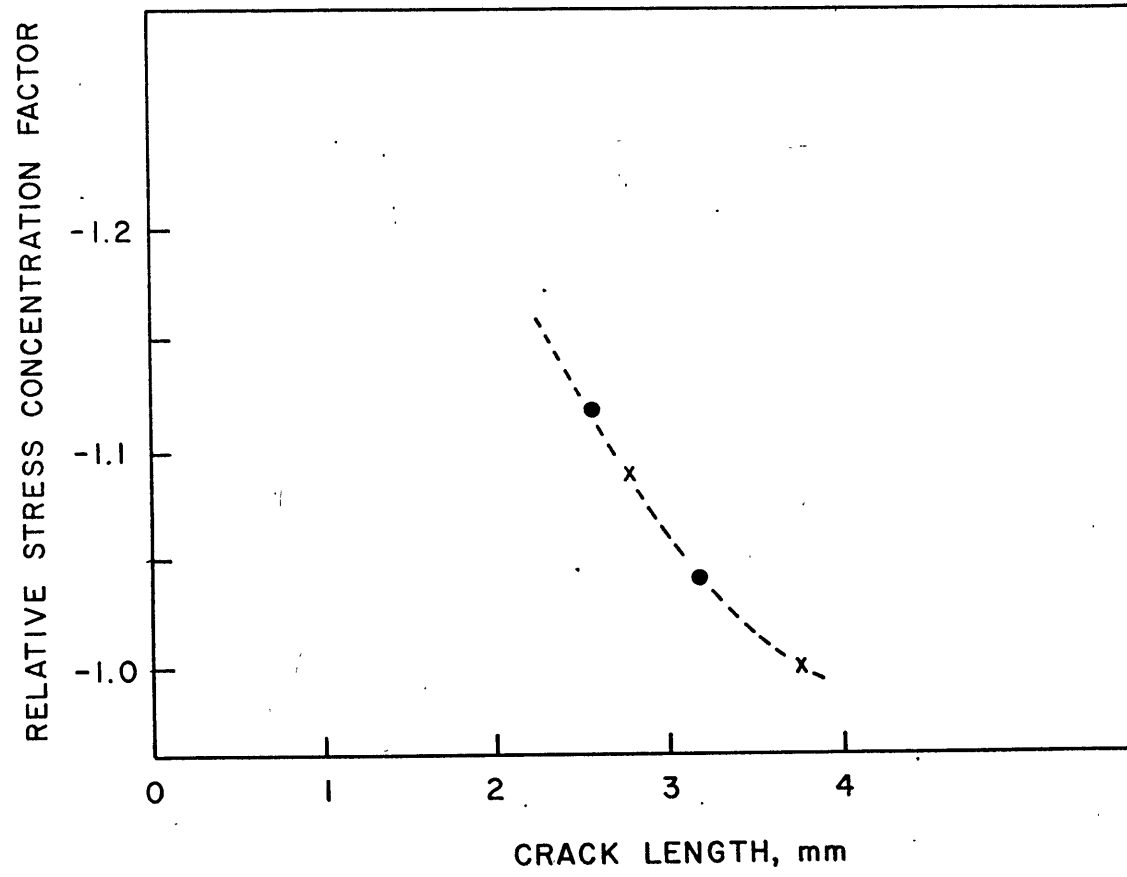
magnitude of the stress concentration factors for crack lengths between 2.76 mm and 3.77 mm.

The results of the two calculations described above have been combined and are illustrated in Figure 16. This diagram is an estimate of the decrease in stress concentration factor with increasing crack length normalized to -1.0 at a crack length of 3.77 mm. The curve was constructed by drawing a straight line between the result obtained from the data in Figure 15. These points are depicted with the solid dots. The other two points, represented by X, were added by constraining the stress concentration factor at 2.77 mm to fall on the straight line between points at crack lengths of 2.57 and 3.17 mm. The curve was then normalized such that the stress concentration factor at 3.77 mm was -1.

Therefore, it appears from Figure 16 that by comparing experiments with initial crack lengths that differ approximately 0.20 mm the difference in stress concentration factors is no more than 3 or 4 per cent. Such small errors are within the experimental scatter of the results and hence will not seriously affect the analysis of the data presented in the text.

Figure 16

Estimated change in relative stress concentration
factor as a function of crack length.



APPENDIX III

TABULATION OF DATA

Stress - 1000 Bars

Partial Pressure of Water - .405 Millibars

Temperature - 153°C

Initial Crack Length - 2.2990 MM.

Time (Sec)	Crack Length (MM.)
------------	--------------------

30	2.5510
90	2.5770
140	2.6120
180	2.6330
240	2.7140
400	2.8380
540	2.9020
1020	3.1010
1200	3.1910
1590	3.2310
1830	3.2490
2500	3.3410
3745	3.4970
5200	3.7240
7200	3.8190

Stress - 780 Bars

Partial Pressure of Water - .405 Millibars

Temperature - 143°C

Initial Crack Length - 2.1880 MM.

Time (Sec)	Crack Length (MM.)
------------	--------------------

85	2.1960
----	--------

270	2.2040
-----	--------

565	2.2240
-----	--------

1430	2.2340
------	--------

2260	2.2550
------	--------

4670	2.2860
------	--------

5870	2.3060
------	--------

13190	2.3230
-------	--------

75000

2.1880

Stress - 930 Bars

Partial Pressure of Water - .405 Millibars

Temperature - 200°C

Initial Crack Length - 2.5760 MM.

Time (Sec)	Crack Length (MM.)
120	2.6450
480	2.7230
990	2.7480
1850	2.7850
2800	2.8100
5400	2.8720
7540	2.9370
10260	2.9620
11880	3.0110
14920	3.0590

Stress - 1000 Bars

Partial Pressure of Water - 405 Millibars

Temperature - 93°C

Initial Crack Length - 2.5250 MM.

Time (Sec)	Crack Length (MM.)
120	2.6020
360	2.6820
540	2.7180
1020	2.7780
1440	2.8230
2460	2.8380
3600	2.8770
5400	2.8990
7440	2.9320
9780	2.9490
14400	2.9810
18480	3.0090
21600	3.0200
28620	3.0640
32700	3.0870
36240	3.1090
39600	3.1210
49200	3.1310
75000	3.1740

Stress - 1000 Bars

Partial Pressure of Water - .405 Millibars

Temperature - 201°C

Initial Crack Length - 3.1740 MM.

Time (Sec)	Crack Length (MM)
60	3.2240
120	3.2580
240	3.3020
300	3.3130
480	3.3380
780	3.3550
1200	3.3850
1560	3.3970
2280	3.4230
3060	3.4600
4560	3.4870
6180	3.5260
7980	3.5450
9180	3.5590
11100	3.6140
12840	3.6540
15000	3.6890
17580	3.7020

Stress - 1000 Bars

Partial Pressure of Water - .405 Millibars

Temperature - 188°C

Initial Crack Length - 2.1890 MM.

Time (Sec)	Crack Length (MM.)
30	2.6230
140	2.9240
180	2.9830
225	3.0260
255	3.0860
290	3.1460
345	3.3850
380	3.4200
410	3.4560
445	3.5000
490	3.5430
515	3.6030
550	3.6630
625	3.7300
665	3.7910
720	3.8230
930	3.8850
980	3.9070
1100	3.9580
1230	4.0090
1380	4.0540
1560	4.0980
1755	4.1520
1980	4.1940

Stress - 1000 Bars

Partial Pressure of Water - 405 Millibars

Temperature - 184°C

Initial Crack Length - 3.6660 MM.

Time (Sec)	Crack Length (MM.)
215	3.7130
800	3.7480
1920	3.7760
2820	3.7880
4440	3.8050
5760	3.8130
7920	3.8210
9180	3.8290

Stress - 890 Bars

Partial Pressure of Water - 15.8 Millibars

Temperature - 128°C

Initial Crack Length - 2.5250 MM.

Time (Sec)	Crack Length (MM.)
30	2.5980
240	2.6540
960	2.6860
1500	2.6940
2760	2.7090
6600	2.7540
7860	2.7690
8820	2.7800

Stress - 890 Bars

Partial Pressure of Water - .60 Millibars

Temperature - 128°C

Initial Crack Length - 2.7870 MM.

Time (Sec)	Crack Length (MM.)
180	2.8230
360	2.8580
480	2.8910
660	2.9350
960	2.9690
2100	3.0580
3000	3.0770
4360	3.1030
4880	3.1260
5760	3.1330
6300	3.1410
13460	3.2540

Stress - 890 Bars

Partial Pressure of Water - .113 Millibars

Temperature - 117°C

Initial Crack Length - 3.2640 MM.

Time (Sec)	Crack Length (MM.)
480	3.2730
1040	3.2920
2420	3.3100
3980	3.3180
5600	3.3340
6860	3.3500
8240	3.3580
10640	3.3740

Stress - 910 Bars

Partial Pressure of Water - .311 Millibars

Temperature - 162°C

Initial Crack Length - 3.5530 MM.

Time (Sec)	Crack Length (MM.)
780	3.5690
960	3.5850
1620	3.5940
2520	3.6030
3240	3.6120
4500	3.6210
5340	3.6300
6480	3.6390
16900	3.7160
26200	3.6870

Stress - 910 Bars

Partial Pressure of Water - 7.6×10^{-4} Millibars

Temperature - 228°C

Initial Crack Length - 3.3200 MM.

Time (Sec)	Crack Length (MM.)
215	3.3310
1175	3.3360
2565	3.3400
4500	3.3450
5520	3.3500
13500	3.3550
18600	3.3590

Stress - 910 Bars

Partial Pressure of Water - 6.1 Millibars

Temperature - 235°C

Initial Crack Length - 3.5200 MM.

Time (Sec)	Crack Length (MM.)
60	3.5570
2820	3.6060
4800	3.6290
6360	3.6570
7500	3.6720

Stress - 910 Bars

Partial Pressure of Water - .045 Millibars

Temperature - 137°C

Initial Crack Length - 2.9740 MM.

Time (Sec)	Crack Length (MM.)
120	2.9910
420	3.0350
780	3.0580
1440	3.0740
3780	3.1060
8220	3.1380
15960	3.1730
17520	3.1820

Stress - 910 Bars

Partial Pressure of Water - 6.2 Millibars

Temperature - 137°C

Initial Crack Length - 3.1820 MM.

Time (Sec)	Crack Length (MM.)
360	3.2000
480	3.2270
600	3.2450
780	3.2620
1320	3.2830
1800	3.3110
2340	3.3330
2880	3.3590
3480	3.3980
4140	3.4360
4780	3.4700
5440	3.4940
5920	3.5290
6220	3.5370
6940	3.5670

Stress - 910 Bars

Partial Pressure of Water - 5.7 Millibars

Temperature - 162°C

Initial Crack Length - 2.6870 MM.

Time (Sec)	Crack Length (MM.)
300	2.7170
780	2.7260
3360	2.7360
6420	2.7460
9600	2.7560
13500	2.7660
19800	2.7750

Stress - 910 Bars

Partial Pressure of Water - .45 Millibars

Temperature - 188°C

Initial Crack Length - 3.0950 MM.

Time (Sec)	Crack Length (MM.)
15	3.2560
60	3.3070
120	3.3420
240	3.3960
420	3.4600
660	3.5000
1080	3.5560
1500	3.5930
1980	3.6490
2760	3.6860
3240	3.7170
3840	3.7480
4500	3.7860
5220	3.8240
6120	3.8550
6780	3.8760

Stress - 910 Bars

Partial Pressure of Water - 6.2 Millibars

Temperature - 188°C

Initial Crack Length - 3.8760 MM.

Time (Sec)	Crack Length (MM.)
60	4.0280
180	4.0860
390	4.2870
600	4.5620
660	4.6440
720	4.7510
840	4.9410
900	5.0650
920	5.1450
970	5.2740
1045	5.4380
1130	5.6470
1185	5.8030

Stress - 655 Bars

Partial Pressure of Water - .45 Millibars

Temperature - 241°C

Initial Crack Length - 2.6210 MM.

Time (Sec)	Crack Length (MM.)
120	2.6530
360	<u>2.6570</u>
840	2.6650
1500	2.6990 ?
2760	2.6820
7380	2.6950
17820	2.7200
28320	2.7370
62880	2.7790

Stress - 740 Bars

Partial Pressure of Water - .45 Millibars

Temperature - 241° C

Initial Crack Length - 2.7790 MM.

Time (Sec)	Crack Length (MM.)
------------	--------------------

60	2.8120
240	2.8440
360	2.8520
540	2.8760
960	2.9070
1380	2.9240
2460	2.9440
2580	2.9630
4940	2.9840
6080	2.9980
8480	3.0180
9800	3.0290
11540	3.0360
12340	3.0480

Stress - 830 Bars

Partial Pressure of Water - .45 Millibars

Temperature - 241° C

Initial Crack Length - 3.0500 MM.

Time (Sec)	Crack Length (MM.)
60	3.0780
90	3.0930
180	3.1580
240	3.2220
360	3.2540
600	3.3020
960	3.3420
1400	3.3690
1780	3.4250
2240	3.4400
2720	3.4770
3440	3.5050
4460	3.5470
5480	3.5680
6620	3.6030
7700	3.6440
9080	3.6830
10280	3.7340

Stress - 970 Bars

Partial Pressure of Water - .45 Millibars

Temperature - 241° C

Initial Crack Length - 3.7420 MM.

Time (Sec)	Crack Length (MM.)
80	3.8180
240	3.8990
360	3.9420
600	3.9910
900	4.0840
1400	4.1320
1640	4.1560
2060	4.2150
2360	4.2370
2780	4.2700
3200	4.3040
3620	4.3150
4040	4.3220
4940	4.3620
5600	4.3760
11000	4.4890

Stress - 980 Bars

Partial Pressure of Water - 0.45 Millibars

Temperature - 241° C

Initial Crack Length - ⁵⁰²4.8280 MM.

Time (Sec) Crack Length (MM.)

60	4.8370
480	4.8630
840	4.8760
1500	4.8920
3780	4.9810
11400	5.1370
23700	5.2820
32700	5.3750
47820	5.5020
121580	5.8000

Stress - 980 Bars

Partial Pressure of Water - .22 Millibars

Temperature - 241° C

Initial Crack Length - 5.8600 MM.

Time (Sec)	Crack Length (MM.)
90	5.9130
150	5.9320
340	5.9670
580	6.0200
1360	6.1900
5440	6.5920

Stress - 525 Bars

Partial Pressure of Water - .405 Millibars

Temperature - 244°C

Initial Crack Length - 2.7810 MM.

Time (Sec)	Crack Length (MM.)
150	2.8130
300	2.8290
480	2.8450
1080	2.8780
1920	2.8950
3000	2.9160
5400	2.9580
7800	2.9780
9720	3.0190
11400	3.0510

Stress - 645 Bars

Partial Pressure of Water - .405 Millibars

Temperature - 244° C

Initial Crack Length - 3.0610 MM.

Time (Sec)	Crack Length (MM.)
30	3.1020
60	3.1280
90	3.1980
180	3.2750
270	3.3460
390	3.4390
540	3.5140
740	3.6160
900	3.6580
1180	3.6960
1420	3.7770
1540	3.8120
1660	3.8320
1840	3.8790
2080	3.9110
2200	3.9650
2380	3.9860
2520	4.0240
2670	4.0490
2850	4.0860
2940	4.1240
3180	4.1730

Stress - 625 Bars

Partial Pressure of Water - .405 Millibars

Temperature - 244^o C

Initial Crack Length - 2.7610 MM.

Time (Sec)	Crack Length (MM.)
60	2.8670
120	2.9090
180	2.9340
240	2.9850
300	3.0260
480	3.0890
600	3.1210
720	3.1540
960	3.2410
1200	3.2780
1380	3.3040
1800	3.3930
2340	3.4440
2700	3.4710
3000	3.5150
3600	3.5820
4140	3.6290
4560	3.6620
5160	3.7160
5760	3.7700

Stress - 625 Bars

Partial Pressure of Water - 405 Millibars

Temperature - 244 °C

Initial Crack Length - 3.7750 MM.

Time (Sec)	Crack Length (MM.)
120	3.7880
300	3.8180
600	3.8430
1020	3.9070
1260	3.9500
1500	3.9620
1800	3.9800
2340	4.0090
3060	4.0580
3660	4.1070
4380	4.1270
5220	4.1570
5820	4.1780

Stress - 695 Bars

Partial Pressure of Water - 405 Millibars

Temperature - 244° C

Initial Crack Length - 4.1780 MM.

Time (Sec)	Crack Length (MM.)
60	4.3250
120	4.4400
180	4.5010
240	4.5640
300	4.6330
390	4.7010
510	4.7830
630	4.8580
675	4.8930
750	4.9230
870	5.0030
990	5.0550
1110	5.1130
1230	5.1770
1410	5.2370
1530	5.2850
1710	5.3630
1950	5.4700
2310	5.6070
2550	5.7080

Stress - 1000 Bars

Partial Pressure of Water - .405 Millibars

Temperature - 100°C

Initial Crack Length - 2.0010 MM.

Time (Sec)	Crack Length (MM.)
60	2.0350
300	2.1010
420	2.1410
720	2.1690
900	2.2070
2580	2.2550
3360	2.2810
4920	2.3060
5880	2.3230
8580	2.3480
11820	2.3620
16740	2.3700
45520	2.3850

Stress - 1060 Bars

Partial Pressure of Water - .405 Millibars

Temperature - 199°C

Initial Crack Length - 3.5930 MM.

Time (Sec) Crack Length (MM.)

120	4.1540
240	4.2340
300	4.3150
420	4.3830
540	4.4330
720	4.4810
840	4.5290
960	4.5560
1200	4.6160
1380	4.6410
1620	4.6980
1860	4.7370
1980	4.7440
2280	4.7840
2580	4.8350
2880	4.8930
3360	4.9620
3780	5.0180
4200	5.0620
4740	5.1100
5340	5.1780
5760	5.2300
6240	5.2820

Stress - 1000 Bars

Partial Pressure of Water - .405 Millibars

Temperature - 100°C

Initial Crack Length - 2.2000 MM.

Time (Sec)	Crack Length (MM.)
30	2.2400
75	2.2880
180	2.3100
420	2.3550
720	2.3990
1380	2.4270
2760	2.4700
3900	2.4840

BIOGRAPHICAL NOTE

NAME: Randolph James Martin III

BORN: July 20, 1942 Waltham, Massachusetts

EDUCATION: Secondary Education: Waltham High School,
Waltham, Massachusetts.

Boston College, 1960 to 1964, B.S.

Massachusetts Institute of Technology, 1964 to present;
M.S. 1968.

PUBLISHED REPORTS:

A test of the law of effective stress for crystalline rocks of low porosity, INT J. Rock, Mech. Min. Sci., Vol. 5, pp. 415-426, 1968, with W.F. Brace.

PROFESSIONAL EXPERIENCE:

In addition to research and teaching assistantship at M.I.T., the author's experience includes the following:

June to September 1963 - NSF stipend to map bedrock geology along the Wachusett Marlborough Tunnel, Massachusetts.

June to September 1964 - Summer Cooperative Program with Geophysical Services Inc., Dallas, Texas.

June to September 1966 - Lecturer in Astronomy, Boston College.

June to September 1967 - Lecturer in Astronomy, Boston College.

June 1968 to February 1969 - Lecturer in Geology, Boston College.

September 1969 to February 1970 - Lecturer in Geology, Boston College.

On March 5, 1966 I married Marie-Therese LaHue and we now have three sons, Michael, Gregory and Matthew.